# A Novel Planar Microstrip Antenna Design for UHF RFID

By

**Madhuri Bharadwaj Eunni**

B.E., Electronics and Communication Engineering,

A.M.A College of Engineering, Kancheepuram –Madras University,

India, May 2004

Master's Thesis

Submitted to the Department of Electrical Engineering and Computer Science and the Faculty of Graduate School of the University of Kansas in partial fulfillment of the requirements for the degree of Master of Science in Electrical Engineering

Thesis Committee

Chair: Dr. Daniel D. Deavours

Dr. Christopher Allen

Dr. Jim Stiles

Date of Defense: July 19, 2006

The Thesis Committee for Madhuri Bharadwaj Eunni certifies

That this is the approved version of the following thesis:

# A Novel Planar Microstrip Antenna Design for UHF RFID

Thesis Committee

Chair: Dr. Daniel D. Deavours

Dr. Christopher Allen

Dr. Jim Stiles

Date Approved: July 19, 2006

## Abstract

**Passive UHF RFID tags suffer from performance degradation when placed near conductors and high dielectric substances. Microstrip RFID tags offer a potential solution to this metal-water problem associated with passive UHF RFID tags. However, their use is limited by narrow bandwidth, manufacturing complexity, because of, the need cross-layered construction and therefore cost. We present a new antenna and matching circuit design using balanced feed that eliminates any reference to ground, provides moderate gain and has broadband impedance matching for low cost metal-mountable RFID tags.**

## Acknowledgements

I would like to thank Information and Telecommunication Technology Center (ITTC) at University of Kansas whose internal commercialization grant helped fund this project.

I am greatly indebted to my advisor, Daniel D. Deavours without whose invaluable guidance and encouragement this thesis could not have been completed. He always showed keen interest in the research process and while encouraging me to explore new ideas freely, gave extremely useful inputs from time to time. His constant effort to understand the underlying principles, and, create better designs has motivated me to do the same. Apart from knowledge of RFID and microstrip antennas that I learnt while working under his guidance, I also had the opportunity to discuss a vast variety of topics with him, though at a rudimentary level. I truly enjoyed being his student and working with him.

I would like to thank Dr. Jim Stiles for being part of my thesis defense committee. As student of Dr. Stiles, I gained a technical insight into the theory of microwave engineering. His teachings have greatly helped me in solving the research questions involved in this thesis. I would also like to thank Dr. Christopher Allen for being a part of my thesis committee and for imparting the know-how need to understand, use, and, design digital circuits, while I was his student. I have used several principles learnt in his class during the implementation stage of this research work.

I would like to thank CReSIS project, its staff, and students, for their technical help and for allowing me to use their equipment.

I would like to express my sincere thanks to Karthik Ramakrishnan; his three hour crash course on RFID helped me start my work. I would also like to thank Padmaja Yatham and Shilpa Sirikonda of the RFID Alliance lab for helping me during measurements. I am especially indebted to my colleague Mutharasu Sivakumar for his continued support during all phases of this research. His penchant for perfection has prevented me from overlooking any important design details. A special thanks to Krishnapriya Kotcherlakota for her expert advice in matters relating to C programming.

I would also like to thank RFID Journal for providing me with the unique experience of attending RFID Journal Live! 2006, an industry conference.

My gratitude towards four very special persons goes beyond words. Without their infinite patience, unconditional love, and, everlasting support none of this would have been possible.

*"When I work on a problem I never think about beauty, but when I have finished, if the solution is not beautiful I know it's wrong".*

*Richard Buckminister Fuller (1895-1983).*

# Table of contents

# List of Figures

# List of Tables

*1.*

# Chapter 1

# Introduction

Auto–ID (automatic identification) technology enables identification and tracking of assets and goods. RFID (Radio frequency identification) has evolved in the recent years as a near ideal implementation of Auto–ID. Most UHF (ultra high frequency) RFID tags are dipoles or some variation of it and thus have characteristics similar to that of a dipole. Dipoles suffer performance degradation when placed near conductors, e.g. metals and high dielectric materials like water. The performance of current RFID tags is therefore limited near such materials. We call this the 'metal-water' problem. Microstrip antennas offer a potential solution to the metal-water problem. The traditional microstrip antenna design principle of a single unbalanced feed requires cross–layered structures. The designs proposed so far based on Planar inverted F (PIFA) [1, 2, 3] are constructed using shorting walls or vias and therefore are of limited commercial viability due to manufacturing complexity and associated costs. The research motivation for this thesis is to determine weather a microstrip antenna that is completely planar can be designed.

This thesis describes the theory, implementation, and discusses the performance characteristics of a planar microstrip antenna with balanced feed and shorting stub matching network. Such a microstrip antenna can be described in its working using traditional odd mode circuit analysis. The planar microstrip antenna is a rectangular patch antenna with two

microstrip transmission feed lines driven 180º out of phase. The antenna is designed on a very low profile substrate, has high performance and is cheap to manufacture.

This thesis is organized into 6 chapters. Chapter 2 deals with background of RFID and related work. It comprises of two major parts, the first part gives a brief introduction to RFID systems; the history of RFID, its current implementation, and standards are presented. In the second part, basics of microstrip antenna along with some common feed techniques and broadband designs are studied. The design of microstrip RFID tags using PIFA, and its limitations are discussed. In chapter 3 we give a detailed description of the theory and working of planar microstrip antenna with balanced feed. The circuit model and odd mode analysis of the antenna are presented. Since this is the first known attempt at construction of a balanced feed microstrip antenna, the effects of various antenna and substrate parameters are studied in detail; an initial set of design parameter values is chosen based on theses studies. Experimental procedures to characterize the materials used in the construction of the planar microstrip antenna are presented. The planar microstrip antenna is designed using these materials with the initial set of parameter values. The design is then optimized to increase performance and reduce form-factor.

Validation of the design by prototype fabrication and experimental measurement of performance characteristics is done and the results are presented in chapter 4. We found that the tag performance does not follow measured gain, and there are also significant differences between measured and simulated antenna gain. Chapter 5 discusses scope of further work

along with some preliminary results for broadband planar microstrip antennas with balanced feed. The conclusions from this work are presented in chapter 6.

*2.*

## Chapter 2

# Background and Related work

The increasing need for security and visibility of goods and assets in manufacturing companies, and, distribution and supply chains has lead to the development of automatic identification systems. Auto-ID and data capture procedures allow identification, data collection, and information storage about assets and goods. Auto-ID techniques include barcodes, lasers, voice recognition, biometrics, and RFID. An ideal Auto-ID technique is one that enables low cost implementation of data transfer without any need for human intervention. Barcodes succeed in this to a large extent, they are however limited in their data storage capability and require LOS (line of sight). The RFID uses IC (integrated circuit) technology that can store large amounts of data, and, RF communication that does not require LOS to overcome these shortcomings. It therefore provides an attractive method of tagging objects and tracking them.

In this chapter we will discuss the history and development of RFID. The key concepts of RFID systems, classification of RFID technology based on its implementation and functionality are presented. Principles of passive UHF RFID operation, its performance characteristics and limitations are studied. Microstrip antennas offer a potential solution to some of these limitations. The basics of microstrip antenna design are presented along with some of the existing microstrip RFID solutions.

## 2.1. Universe of RFID

Since its first use in the1930s, RFID technology has expanded and developed into mainstream consumer good identification and tracking application. Being technically superior to other mechanisms like bar codes [4][5], it enables RFID tagged goods to be detected without the need for physical contact or LOS; combined with other advantages like increased storage, greater accuracy and reliability has made this an attractive Auto-ID solution [5]. Over the years RFID has evolved to meet the industry needs, resulting in numerous specifications and standards.

### 2.1.1. History of RFID

RFID technology although has found implementations in tracking supplies in the late 80's it has been in existence since 1939 when it was first used as IFF (Identify Friend or Foe). IFF was a tag and track (i.e: to tag an object and track its movement) technique used by the British allies to identify whether airplanes were friend or foe [8]. 1960s and 70s RFID tags found military applications like equipment and personnel tracking [7] and some unique commercial applications like identification and temperature sensing of cattle. However the major development in RFID tracking came only in the 80s and 90s when industrial goods needed counterfeit protection, shrinkage protection and tracking through the several stages in the supply chain. RFID technology prevents theft or counterfeiting of goods thus providing security, automatic counting of goods that enter or leave warehouses allows us to keep a track of the stock levels. Passive UHF RFID systems are increasingly being employed in distribution and supply chains like Wal-mart and Tesco [6]. Recently several government agencies including US-DOD and FDA have issued mandates requiring suppliers to use RFID

on their products [9] [10]. Apart from the industrial applications, RFID was used for baggage tracking and access control.

With the popularity of RFID in the industry and the proven advantage of real time tracking of goods, several manufacturers started to use the technology, there was a necessity for compatibility between tags and readers, and hence the focus of work shifted to setting industry driven standards for using RFID in supply chains. EPCgobal Inc., is leading this standardization [11].

### 2.1.2. Need for RFID

Auto–ID technology is implemented in several different ways, including barcodes, lasers, voice recognition, and, biometrics. These techniques suffer from limitations like the need for LOS with the interrogator (lasers and barcodes), low data storage capacities (barcodes), and need for human intervention (voice recognition and biometrics). RFID was developed to overcome these limitations. RFID provides an Auto-ID technology that can operate without a LOS, can store large amounts of user data using integrated technology. RFID proves useful when traceability through process or life cycles is required; data errors are high in material identification or handling; and where business systems need more information than automatic identification technologies like bar coding can provide [5].

### 2.1.3. Types of RFID

The main components of any RFID system are the tag, the reader and the host computer. RFID tags can be classified into two major categories based on how a tag stores the data that has to be identified. They are without an Integrated Circuit (IC) chip or with an IC chip. The former is a tag that has unique patterns printed on the surface of the material that corresponds to a certain code or data that is to be stored when read by the reader. A good example of this is a SAW RFID – surface acoustic wave RFID which is based on the dispersion of low speed acoustic waves from the surface of a material and on piezoelectric effect. These tags are read only, with a unique number, which is in a way similar to bar codes. SAW RFID systems are used in high temperatures, x-rays or gamma rays [12] and heavy manufacturing environments [13]. The second is a type of RFID that has an IC. The IC contains all the necessary data to uniquely identify an object. The IC derives its power from the RF signal incident on it from the reader and communicates back to the reader. The different classes of UHF RFID tags are discussed under Section 2.1.5

### 2.1.4. Implementation of RFID to asset identification and tracking

RFID system is made of three major components, the reader or interrogator, the tag or transponder, and the host computer. The reader is connected to the host computer which is used to program the reader and store information received from the transponder. The transponder is placed on the object to be identified. The reader is a radio transceiver [14] connected to transmit and receive antennas. The tag consists of an antenna and the RFID IC that contains data. The block representation of a RFID system is shown in Figure 2.1.

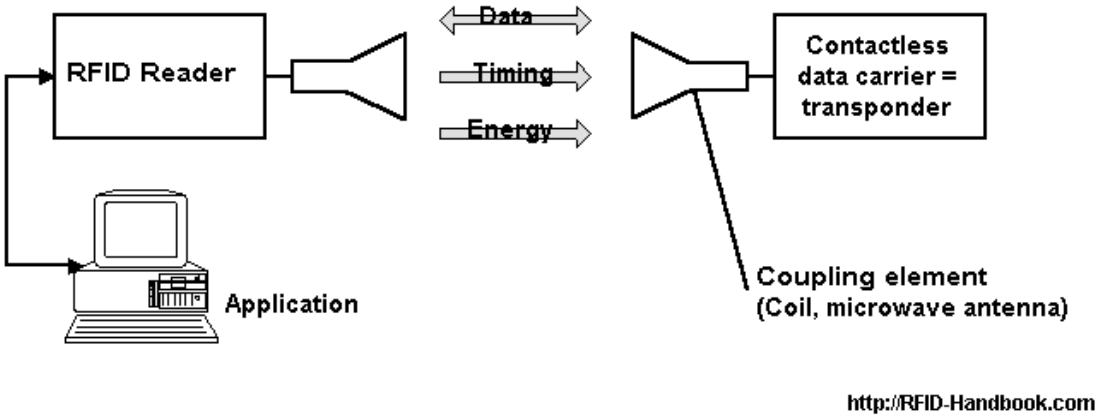


Figure 2.1: RFID system block representation taken from RFID handbook [15]

### 2.1.5. Existing technologies

RFID systems can be designed to operate from Low frequency (LF) to Super high frequency (SHF); their operation is regulated to avoid interference with other Electromagnetic (EM) devices. The unlicensed Industrial-Scientific-Medical (ISM) and Short-Range Devices (SRD) frequencies bands that are used for RFID are summarized in table 2.1 [15]

| Frequency range | Description |
|---|---|
| < 135 kHz | Low frequency |
| 6.765 - 6.795 MHz | Medium frequency (ISM) |
| 7.400 - 8.800 MHz | Medium frequency, used for EAS |
| 13.553 - 13.567 MHz | Medium frequency (13.56 MHz, ISM – contact less smartcards, cattle, and, asset tracking, and several other applications |
| 26.957- 27.283 MHz | Medium frequency |
| 433 MHz | UHF (ISM) rarely used for RFID |
| 868-870 MHz | UHF (SRD) |
| 902 - 928 MHz | UHF (SRD) widely used |

| | |
|---|---|
| 2.400 - 2.483 GHz | SHF (ISM), vehicle identification |
| 5.725 - 5.875 GHz | SHF (ISM), rarely used for passive RFID, active tags commonly use these frequencies |

Table 2.1: RFID system block representation taken from RFID handbook [5]

RFID uses electromagnetic wave propagation to transmit and receive data. Chip based RFID can be implemented in different ways- passive, semi-passive, active. The operating principle for tag–reader communication is either inductive coupling between the reader and the tag or backscattering. Inductive coupling is the transfer of energy from one device to another through a shared magnetic field [16]. The reflection of electromagnetic waves back in the direction from which they were received is called backscattering.

Near field RFID are based on inductive coupling between the reader and the tag. It is used where the distance between the tag and the reader is on the order of the free space wavelength. The magnetic field induction between the reader and tag enables communication. Near field RFID is commonly operated in low and medium frequency bands. Far field RFID uses backscattering

The classification of UHF RFID tags based on their operation and functionality was developed by the Auto-ID center [17]. The layered class structure divides the tags from class 0 through class 5 as detailed below.

- Class 0 are passive read only tags. They use out of band signaling [18] and use back-scatter technique to communicate to the reader.

- Class 1 are also passive read only tags, but they are the program-once- read-many type tags, wherein the programming of the tag can be either done by the manufacturer or the user, but only once. The tags use in band signaling [18] and backscattering

- Class 2 are passive tags that have the additional capability of storage and encryption [14]. Use backscattering to communicate with reader.

- Class 3 are semi passive tags that have a battery source to operate the internal circuitry. However they do not have a transmitter to send across signals to other tags / readers. They also use backscattering for reader communication.

- Class 4 tags have a battery source to supply power to the internal circuitry and have a transmitter too. These tags are also capable of communicating with other tags that have the same technology.

- Class 5 tags, again are active, and have the additional capability of successfully powering other IC's of peer class and lower classes and can have two way communication with class 4 tags. RFID readers may come under this category.

In the next section we will discuss the operating principle and performance characteristics of UHF RFID systems.

## 2.2. Passive UHF RFID

Passive UHF RFID is operated in different segments of the 860-960MHz ISM band in different countries (see Appendix – A for detailed description of frequencies of operation in

different countries). In section 2.1.4 we showed that electromagnetic wave propagation is used to communicate between the tag and the reader. In passive UHF RFID systems, the reader, primarily as a transmitter, transmits RF energy to sense the tag, a tag consisting of a tuned antenna and a load (i.e. the RFID IC) in the far-field of the transmitter acts as a receiver and receives the RF energy from the tag. If there is sufficient energy to power up the RFID IC, then the tag responds to the reader. The RF energy from the reader to the tag (forward link) is backscattered from the tag to the reader (reverse link) along with data from the RFID IC. The ability of the tag to receive RF energy and efficiency backscatter it depends on antenna characteristics and channel properties. The operating principles and the typical characteristics of UHF RFID tags are detailed below.

### 2.2.1. Electromagnetics of RFID

The most common implementation of passive UHF RFID tag antenna is using a simple dipole or some variation of it e.g., dual dipole, folded dipole [19] [21]. The dipole is made an efficient radiator by designing it to be odd multiples of $\lambda / 2$ in length where, $\lambda$ is the wavelength at the central operating frequency. The tag performance, however, depends on the radiation characteristics and the power transfer between the tag antenna and the RFID IC.

If an antenna is considered as a device that accepts power from one device and radiates it into space, then the radiation efficiency of an antenna can be defined as the ratio of power radiated into space to the total power accepted [19, 20]. It is also known as antenna efficiency.

$$P_{radiated} = P_{accepted} * \eta \quad (2.1)$$

Not all the power accepted by the antenna can be radiated by it, some power is lost as it is either absorbed by the substrate (dielectric losses) or ground (ground losses) or converted in to heat.

A tag antenna can have good radiation efficiency and still be poor in performance if there is considerable mismatch between the load and the antenna impedance. In RFID tags the load is the RFID IC. A mismatch will result in RF energy being reflected back to the transmitter without powering up the RFID IC. Therefore, it is important to match the antenna impedance to the complex conjugate to the RFID IC impedance to achieve good power transfer from the antenna to the load. By definition [19], the gain of an antenna (usually expressed in dBi) is the ratio the energy radiated in particular direction when the antenna is excited with a certain amount of input power to the theoretical isotropic antenna excited with the same amount. Gain of the antenna takes both the radiation efficiency and the impedance match into account. This is discussed in greater detail in chapter 3.

Assuming that the RFID system is operated in an ideal channel environment, Friis equations [19, 21] can be used to determine the power received from the reader to the tag for a given distance.

$$P_r = \frac{P_t G_t G_r \lambda^2}{(4\pi r)^2} \tag{2.2}$$

Where $P_r$ is the power received from reader antenna to the tag antenna. It is calculated at a distance $r$ from the reader. The power transmitted by the reader is given by $P_t$. The reader and tag antenna gains are given by $G_t$ and $G_r$ respectively.

In real applications however, there could be polarization mismatch ($p$) between the reader and the tag antennas, and also not all power absorbed by the receiver is available to the load due to impedance mismatch ($q$). Taking these factors into consideration the modified Friis equation is written as shown in equation 2.3

$$P_r = pq\frac{P_t G_t G_r \lambda^2}{(4\pi r)^2} \tag{2.3}$$

The received power is used to both power up the RFID IC and re-radiate to the reader. The RFID IC load varies from being nearly perfectly matched to the antenna impedance allowing power transfer between the IC and the antenna; to a mismatched condition when all the power is backscattered to the reader. External factors such as channel attenuation, multipath, properties of the materials to which the tag is attached can change the overall tag performance.

### 2.2.2. General characteristics

The performance of RFID tags vary depending on the conditions in which it is used. The general characteristics of commercially available passive UHF RFID tags based on performance benchmarks for passive UHF RFID tags by [14] are summarized below.

- *Performance in free space:* Performance metric of a tag is measured in terms of the number of times a tag responds to the reader and is detected or read by it. The number of successful reads per unit time is defined as read rate or response rate. Most tags perform well when measured in free space. The read rate deceases as we move farther in distance since attenuation increases. The decrease in read rate is dependent on Friis transmission equations. Another performance metric is the orientation sensitivity of tags. Single dipole tags are more sensitive to orientation than dual dipole designs due to difference in radiation patterns.

- *Variance in tags:* Typically tags exhibit considerable variance in performance. The lowest variance measured by [14] was nearly 3dB.

- *Read rates:* Different protocols result in different read responses in isolation and in population. Where isolation is defined as a condition in which only one tag is present in the reader RF field and population means when a certain number of tags are all simultaneously present within the reader RF field.

- *Performance near metal:* Tags under go severe performance degradation when placed in front of metal. It was observed that all tags tested would be read at 2.5mm separation from metal. As separation increases performance improves.

- *Performance near water:* Most tags get detuned in front of water. The tags that perform well in free space do necessarily perform well near water. According to [14] that all tags tested would be read at 2.5mm separation from metal. As separation increases performance improved.

- *Performance near water:* Most tags are de-tuned near water. Tags that perform well in free space do not necessarily perform well near water.

The above studies [14] show that passive RFID tags are limited in performance depending on external factors such as distance, orientation and tagged material properties.

### 2.2.3. Performance limitations

It was noted in the previous section that most RFID tags perform well in free space, but undergo performance degradation when attached to different materials. This loss of performance is because the material characteristics affect critical antenna properties such as substrate dielectric constant and loss tangent, radiation efficiency, radiation pattern, and radiation impedance.

High dielectric and lossy materials such as water detune the tag and reduce radiation efficiency. Proximity to metals causes large increase in the antenna radiation resistance

which prevents efficient power transfer between the antenna and the RFID IC. Since metal and water are common materials that RFID is commonly used to track, we call this the metal-water problem. Using low dielectric materials like foam and plastics to separate metals can improve tag performance, but it also increases thickness and manufacturing costs significantly. Moreover, plastics that have low dielectric constant and low loss can still detune the antenna, though modestly, by changing the substrate properties. Figure 2.2 shows the effect of different materials on dipole far-field radiation efficiency.

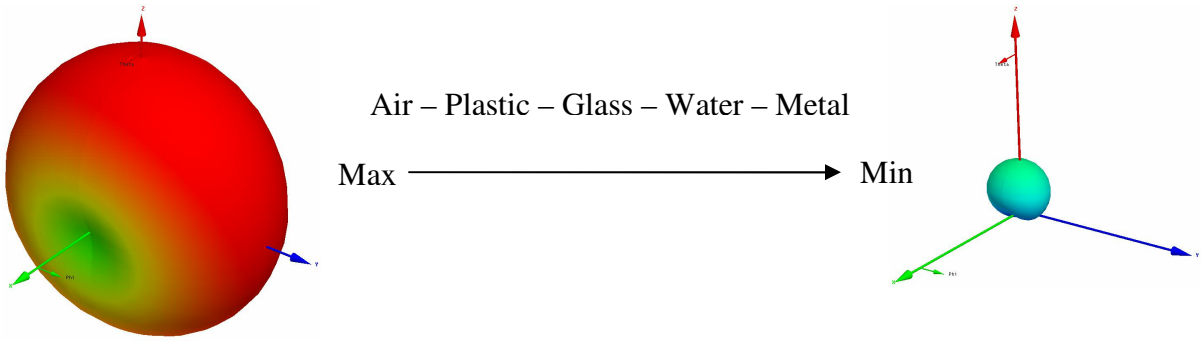


Figure 2.2: Qualitative performance degradation of a UHF dipole when placed on different materials.

The tendency of RFID tags to lose performance when attached to certain materials limits its application to tagging materials that have nearly free space properties. Unfortunately, most assets are metal made, are encased in plastic containers or metal containers. Therefore there is an immediate need to develop RFID tags that will have consistent performance characteristics irrespective of the material to which it is attached.

While several attempts [23, 24, 25] have been made to create tags that perform well when attached to metal or plastics. They are mostly, specific models that are pre-tuned to work on different materials [24, 25]. For example a tag designed to work well near metal will still be de-tuned when placed on plastic or near water. Or they are ordinary dipoles or some

variation of it encased in rugged plastic cases to shield from the effects of metal and water. One way to achieve uniform performance with different materials is to design an antenna that is electrically separated from the material. Microstrip antennas have a top antenna layer a substrate and a ground plane. The ground plane separates the microstrip antenna from the material to which it is attached. Microstrip antennas thus offer a potential the metal-water problem of passive UHF RFID.

## 2.3. Literature survey of microstrip antennas

Originally implemented in 1950's [26] microstrip antennas have since been researched extensively. The inherent advantages like low profile, lightweight, and, low fabrication cost [36] along with ease of fabrication and integration with other microwave microstrip devices, has lead to numerous industrial applications for microstrip antennas. In this section the basics of microstrip antenna along with a brief introduction to some of the feed mechanisms and broadband techniques is presented. Recently microstrip antennas have been used to overcome the problems associated with passive UHF RFID tags; these implementations are discussed in Section 2.3.4.

### 2.3.1. Basics of microstrip antenna design

In its simplest form a microstrip antenna consists of a dielectric substrate sandwiched between two conducting surfaces: the antenna plane and the ground plane. The simplified microstrip patch antenna is shown in Figure 2.3.

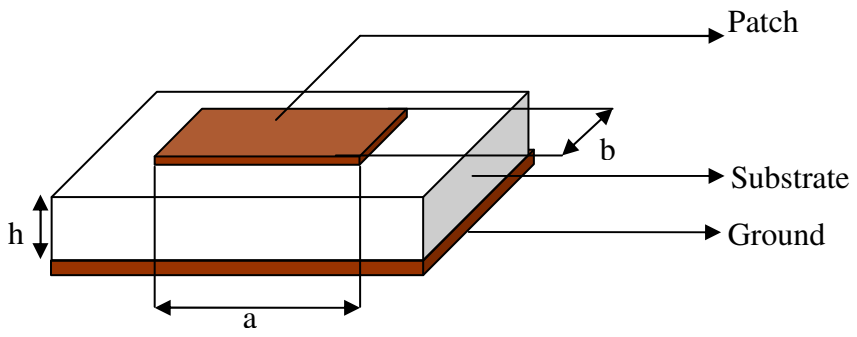


Figure 2.3: Basic rectangular microstrip patch antenna construction.

Microstrip patch antennas radiate primarily because of the fringing fields between the patch edge and the ground plane. Since the propagating EM fields lie, both in the substrate and in free space, a quasi-TEM mode is generated. The length and width of the patch are given by a and b respectively. The substrate thickness is given by h. When the dimension along a is greater than b TM10 mode is the fundamental resonant mode and TM01 is secondary. If dimension along b is greater than a then the order is reversed.

Two of the most common methods for describing the working of microstrip antennas are the transmission line model [28, 29] and the cavity model [30, 31]. The transmission line model is the simplest and sufficiently accurate in calculating the input impedances for simple geometries. Its use, however, is limited by inaccuracies in prediction of impedance bandwidth and radiation patterns, especially when thin substrates are used. The cavity model [28, 29] assumes the antenna and ground planes to be electrical plates and the patch edges to be surrounded by magnetic walls. This model is more accurate but computational complex when compared to the transmission line model.

Microstrip antenna performance is affected by the patch geometry, substrate properties and feed techniques. One of the advantages of microstrip antennas is the freedom to choose from a variety of patch geometries. Square patch (a = b) geometries allow both TM10 and TM01 modes to occur at the same frequency, this can be used to design λ / 4 antennas, Slight difference between the length and width (a ≠ b) can induce circular polarization. Some of the commonly used geometries are: square, rectangle, dipole, circle, annulus, and, triangle.

A dielectric substrate with properties such as low loss, low dielectric, and sufficiently thick substrate can provide maximum radiation efficiency and bandwidth. However, the antenna dimensions are large when low dielectric substrates are used. Low loss substrates provide good radiation efficiency, but also make the microstrip antenna a high-Q device, resulting in narrow bandwidth. The use of high dielectric substrates with higher loss gives reduced performance, but greater bandwidth and smaller dimensions. The effects of substrate properties on microstrip antennas and the tradeoffs involved are discussed in detail in section 3.3.

### 2.3.2. Feed mechanisms

A number of feed mechanisms have been developed for microstrip antennas [19, 32]. Most often it is the feed mechanism that determines the complexity of the microstrip antenna design. Popular feed techniques can be classified into two broad categories as follows.

- Directly connected to patch: A direct electrical connection is used to feed the radiating patch element. E.g., microstrip line, coaxial probe.

Microstrip Line Feed is one of the most commonly used feed technique; a conducting strip is connected directly to the edge of the microstrip patch. Inset feed is one in which the microstrip line feed is inset into the patch [32] to provide the right impedance match between the patch and the feed line; refer Figure 2.4a. The advantage of this technique is that both the feed and the patch lie on the surface of the substrate and therefore is planar in construction. This technique is efficient on thin substrates; thick substrates should be avoided as they could result in spurious feed radiation and cross polarization effects.

The Coaxial feed or probe feed has the inner conductor connected of the coaxial cable to the patch through a hole in the substrate and the outer shield grounded by connecting to the microstrip ground plane; see figure 2.4b. Though it is easy to place the feed at any location on the patch, the disadvantage with this technique is it provides narrow impedance bandwidth and is difficult to model [33, 34].

- Coupled to the patch: Electromagnetic field coupling is used to feed the patch. E.g., aperture coupling and proximity.

In Aperture Coupled Feed the feed line is separated from the patch by the ground plane. Electromagnetic coupling is used to transfer power from the feed line to the patch through a slot in the ground plane. To avoid cross-polarization the coupling aperture is centered under the patch as shown in Figure 2.4c. It is a multi-layered

design, the efficiency of aperture coupling is lower compared to other techniques, but it is easy to model [35].

Proximity coupling feed has a feed line sandwiched between two different substrates, see figure 2.4d. The microstrip antenna is on the top dielectric and the ground plane is on the bottom dielectric slab. The feed line is placed between the two dielectric slabs. The coupling is primarily capactive in nature [35].This feed mechanism provides greater than 13% fractional bandwidth [19, 35]. The fabrication complexity however is greater than any of the previous designs.

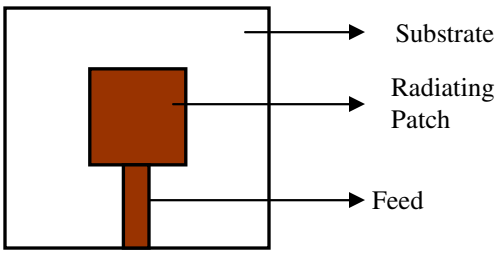


Figure 2.4a: Microstripline feed

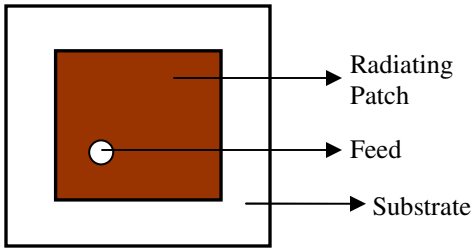


Figure 2.4b: Coaxial probe feed

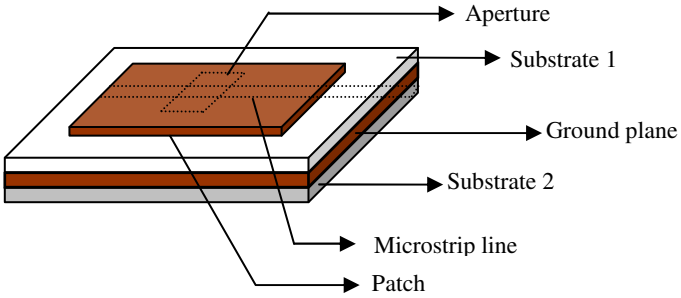


Figure 2.4c: Aperture coupling

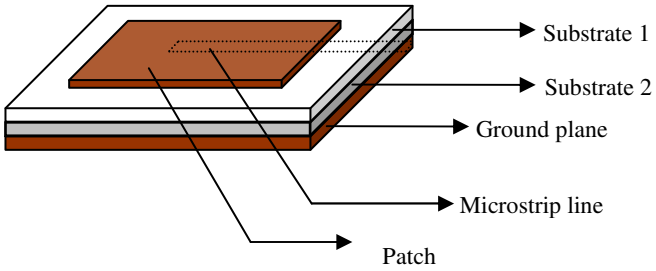

Figure 2.4d: Proximity coupling

Along with a number of advantages [33] microstrip antennas also suffer from some disadvantages [32, 34] like narrow bandwidth, low efficiency, low Gain, spurious radiation and surface wave excitation. While spurious radiation and surface waves can be eliminated by using the right feed mechanisms and substrate thickness [32], the issues of major concern are poor bandwidth and low radiation efficiency. Microstrip antennas inherently suffer from Ohmic losses, and dielectric losses making it a high Q device [32]. In order to achieve greater bandwidth and gain we must increase substrate thickness but this could result in surface waves, therefore alternate methods are explored [34].

### 2.3.3. Broadband antennas

Microstrip antennas are generally capable of 2 - 7% fractional bandwidth [36]. Passive UHF RFID tags are operated in different frequencies bands from 860 – 960 MHz across the world, see Appendix A for detailed frequency of operation in different countries. Microstrip passive UHF RFID tags therefore require a fractional bandwidth of 10.9% to operate in all these countries. To increase the microstrip antenna bandwidth, techniques such as increasing dielectric height, proximity coupling feed techniques, perturbing the patch geometry to create multiple resonances, coupled or stacked patches and antenna arrays are used [34].

Some the advantages and disadvantages of these techniques, discussed in [34] are summarized below.

Increasing dielectric height is the simplest way to increase antenna bandwidth, but it causes surface wave excitation and increase in antenna profile. Proximity coupled feed requires the use of two substrates that increases overall antenna thickness and is not easy to fabricate. Perturbation of the patch geometry is one of the most effective ways to increase antenna bandwidth without increase in profile or form-factor. The radiating patch is designed such that it can generate $TM_{10}$ and $TM_{01}$ modes at the desired frequencies. Slots in the radiating patch can be used to meander currents and create multiple resonances. Two microstrip patches of different lengths can be placed in proximity with each other such that they are critically coupled and excited with a single feed. This will result in a dual band resonance.

Having two dielectric substrates with a patch on each one of them and stacking them one on top of the other with a single ground plane at the bottom gives a stacked patch. This can be designed to give dual or quad band resonances [36]. It however necessitates significant increase in antenna profile. The concept of coupled and stacked patches can be extended to more than two resonances. When larger bandwidth and increased gain are required a number of antenna elements are connected to gather top form an array that will result in greater aperture and consequently larger gain and bandwidth. The use of larger number of elements however increases the antenna size.

It is evident from the above techniques that any increase the bandwidth or efficiency of a microstrip antenna is accompanied by increase in size or thickness of the antenna.

### 2.3.4. Existing microstrip RFID designs

Researchers in the recent years have explored several microstrip antenna designs towards RFID implementation [1, 2, 3, 27]. The inverted-F microstrip antenna forms the basis for most of these designs. The inverted F antenna [37] is constructed by a quarterwavelength patch terminated at on end with shorting wall or pins connecting it to the ground plane. The patch extends from the top antenna plane with a right angle bend to the ground plane, the ground enclosed structure looks like an inverted – F.

Planar inverted F antennas of reduced size and good performance for RFID tags were proposed in [2, 3]. The PIFA is feed with a wire connected to the ground plane [3] as shown in Figure 2.5, and hence is called wire-type PIFA. This type of a construction requires imbedding the RFID IC vertically between the ground plane and the radiating patch. The manufacturing complexity for this type of construction is significant, and prevents the design from becoming a viable commercial solution for UHF RFID applications.

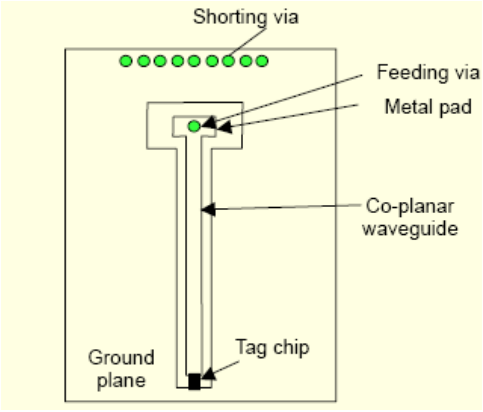


Figure 2.5: Chip attached to PIFA RFID tag [3].

An improvement to the above design was suggested by [1] in which slotted PIFA was designed. The shorting pins are replaced with a continuous metal shorting wall that extends

half way into the substrate. The design has a 'U-shaped' slot in the patch. RFID IC is now surface mounted, see Figure 2.6. Though this design is an improvement in some ways compared to the wire-type PIFA, it still requires a 3-D construction.

Current RFID tag technology uses simple tag manufacturing techniques. The tag antenna is printed or etched on an inlay, and the RFID IC is attached to the antenna. The inlay is then attached to a substrate with adhesive. In order to be easily incorporated into such a manufacturing process the microstrip antenna design must allow surface mounting of the RFID IC and also be free of any cross-layered structures such as vias or shorting walls.

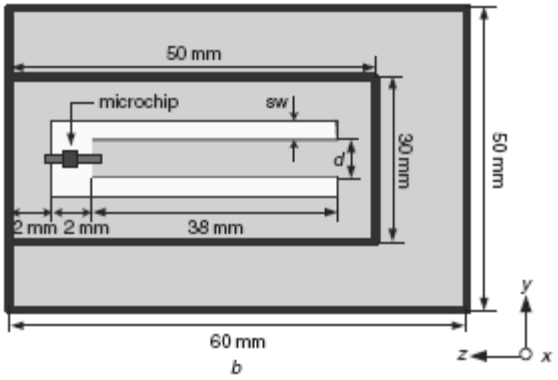


Figure 2.6: Slotted PIFA design with surface chip attachment [1]

The design of planar microstrip antenna with balanced feed presented in this thesis achieves this goal. The theory and design details of this are presented in the following chapter.

*3.*

# Chapter 3
# Implementation

Traditionally microstrip antennas are viewed as unbalanced devices. A microstrip feed is single feed that can be designed as probe feed, microstrip line feed, or aperture feed and the reference is always with respect to the ground plane. We reviewed some of these techniques in chapter 2. With respect to RFID applications, the disadvantage with these feed techniques is that they require a cross - layered construction such as a via or a shorting wall in order to attach an RFID IC. Microstrip RFID tags discussed in Section 2.3.4 are significantly complex and costly to construct.

In contrast, we view the microstrip antenna as capable of balanced feed. We present here a completely planar microstrip RFID tag design. This implementation does not require any cross-layered structures and hence greatly simplifies tag construction and consequently the cost associated with it. The new antenna and the matching circuit design using the balanced feed approach eliminates any reference to ground. The tag is constructed using readily available materials that are experimentally characterized.

In the following sections we discuss the method of approach for creating a balanced feed from two unbalanced microstrip transmission lines. Since the two lines have odd mode symmetry, traditional odd-mode analysis is used to describe the antenna and matching circuit. This is followed by characterization of construction materials i.e. dielectric and loss tangent of substrate and impedance of the RFID IC. The remainder of chapter 3 discusses the

design parameters and the evolution of the tag design from a dual stub matching network design to the optimized model. All simulations were done using Ansoft Designer. The simulation results for each implementation are also presented. Bandwidth of the tag and its form factor continue to be the limiting factors in the tag performance, these issues are addressed towards the end of the chapter.

## 3.1. Balanced feed matching network design

Unlike existing techniques that use a single feed line to the microstrip patch the premise of our approach is that we use two feeds i.e. two unbalanced transmission lines to effectively create a single (virtual) balanced transmission line feed structure and thus eliminate any cross- layered structures.

### 3.1.1. Approach

Microstrip patches offer the ability to construct antennas with the feed on a single surface by use of microstripline feed. A microstripline feed connects to the patch either on the radiating or the non-radiating edge and the position of the microstripline is adjusted relative to the patch to achieve the desired input impedance (refer section 2.4.2). In the following example we chose a single shorted tuning stub for impedance matching. Let us consider a simple rectangular microstrip patch antenna as shown in Figure 3.1a with a single microstripline feed that can be connect directly to an unbalanced device. The RFID IC, however, is balanced device with two ports; each port is 180º out of phase with respect to the other. Therefore, for a single feed design one end of the RFID IC is attached to the microstrip line

while the other end is grounded using a via. The position and the length of the stub determine the reactive component of the overall impedance.

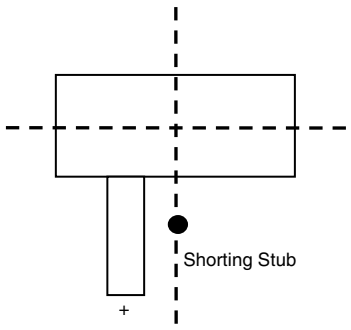


Figure 3.1a: Single microstripline unbalanced feed with shorting stub.

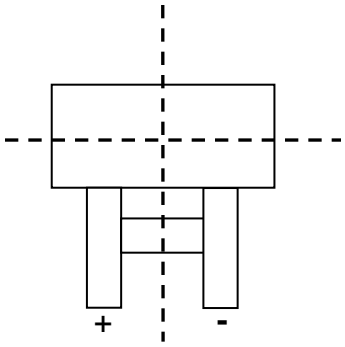


Figure 3.1b: Dual microstripline differential feed with shorting stub.

Now, instead of using a single microstripline feed, we use two feeds connected symmetrically about the vertical central axis of the patch as seen in figure 3.1b. The differential feed to the patch antenna is achieved by using the two symmetric feed lines. The RFID IC is connected to the two feeds. In our case, since both the feed lines need to be matched we must either use two matching networks or simply construct a matching network connected to both the feed lines. The shorting stub is extended symmetrically to connect with the second feed line. Observe that figure 3.1b has E-plane symmetry. The vertical dotted line represents the axis of symmetry. The rectangular patch is equivalent of a transmission line with characteristic impedance $Z_A$. Therefore the current and voltage distributions along the patch antenna is same as that long a open ended transmission line given by

$$I(x) = I_o \sin\left(\frac{2\pi x}{\lambda}\right) e^{jw} \qquad \text{where } I_o \text{ is the current at } x = 0 \text{ and } x \text{ the distance in terms of } \lambda \tag{3.1}$$

$$V(x) = V_o \cos\left(\frac{2\pi x}{\lambda}\right) e^{jw} \qquad \text{where } V_o \text{ is the voltage at } x = 0 \tag{3.2}$$

From the above equations the current and voltage distributions along a λ / 2 transmission line is shown in Figures 3.2 and 3.3.

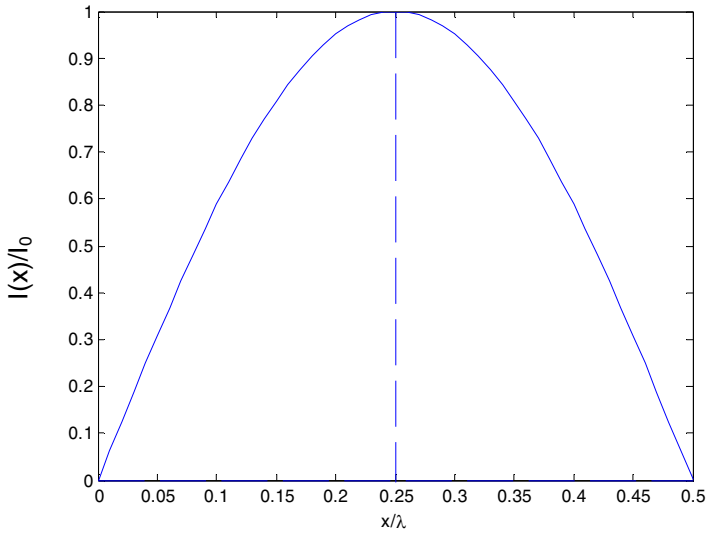


Figure 3.2: Current distribution vs. distance along a transmission line section.

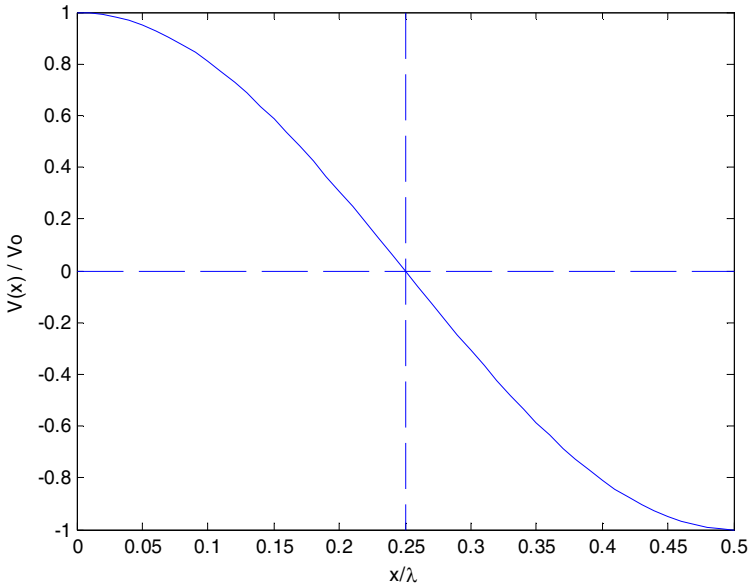


Figure 3.3: Voltage distribution vs. distance along a transmission line section.

The impedance along the transmission line is given by equation 3.3

$$Z(x) = \left( \frac{V(x)}{I(x)} \right)$$

The RFID microstrip tag acts as a receiver. If we consider the microstrip tag with a rectangular patch antenna the circuit model of the rectangular patch is as shown in Figure 3.4.

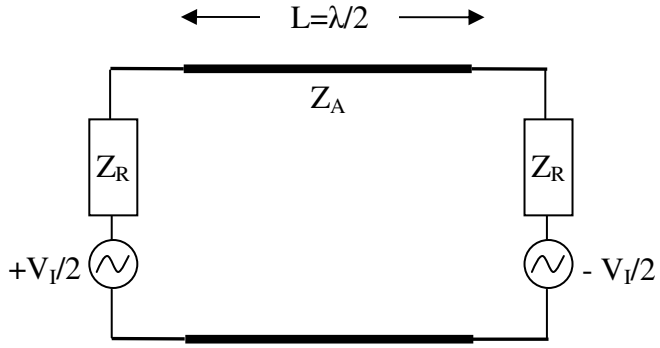


Figure 3.4: Circuit model of a rectangular microstrip patch.

The total patch length is λ / 2, and, the radiating impedance is given by $Z_R$. Since the patch is considered to receive RF energy from the reader, the induced voltage on the patch is represented by $V_I$. From equations 3.2, 3.3 and 3.4 we that at x = λ / 4 the impedance goes to zero creating a virtual ground at the center of the rectangular patch. Combining the facts that the microstrip antenna with a balanced feed matching network has E-plane symmetry (refer Figure 3.1b) and that the line of symmetry at x = λ / 4 is a virtual ground, (Figure 3.2 and 3.3) even-odd mode analysis can be used to describe the working of the antenna and the matching network.

**Circuit analysis**

From figures 3.1b and 3.4 we observe that the patch antenna has E-plane symmetry and is represented by two sections of λ / 4 length transmission line sections. In order to make the

circuit completely symmetric about the vertical axis the induced voltage is divided into two equal halves across plane of. The circuit model is then given by Figure 3.5.

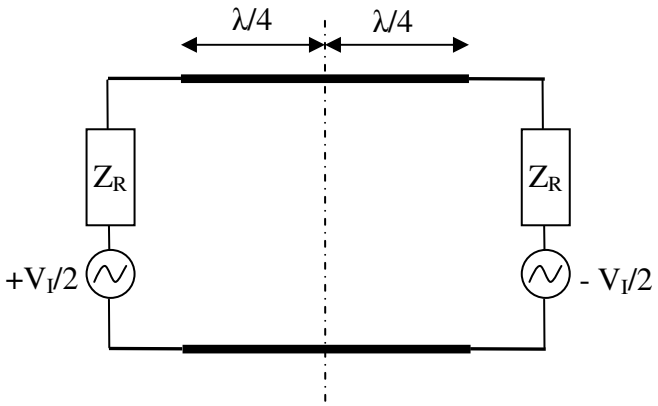


Figure 3.5: Circuit model of a rectangular microstrip patch with plane of symmetry.

The even and odd modes representations for the above circuit are shown in Figures 3.6 and 3.7 respectively.

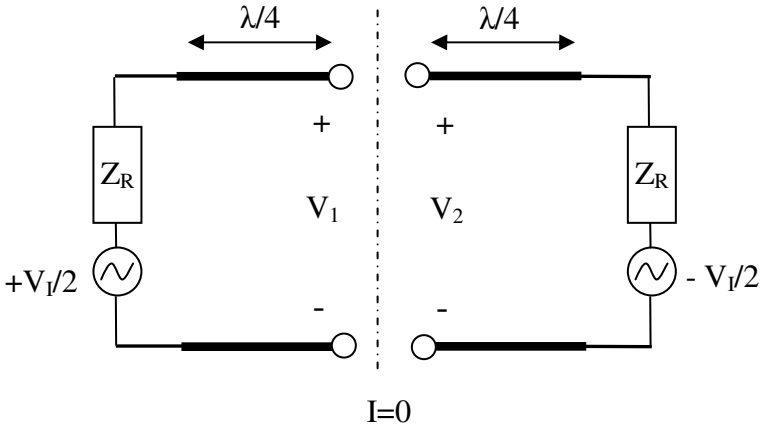


Figure 3.6: Even mode symmetry circuit model.

The rectangular patch is a λ / 2 transmission line section with both ends having open circuit. Applying boundary conditions to this the fundamental solution is where axis of symmetry is a short circuit. Even mode symmetry does not satisfy these conditions. In even mode the axis

of symmetry is an open circuit. The current flow due to even mode does not contribute to the radiation of the rectangular patch. The voltages $V_1$ and $V_2$ are both equal to zero. The even mode is therefore trivial. Also we now from the current and voltage distributions that the axis is symmetry is a short circuit. Therefore odd mode analysis alone is sufficient to describe this circuit.

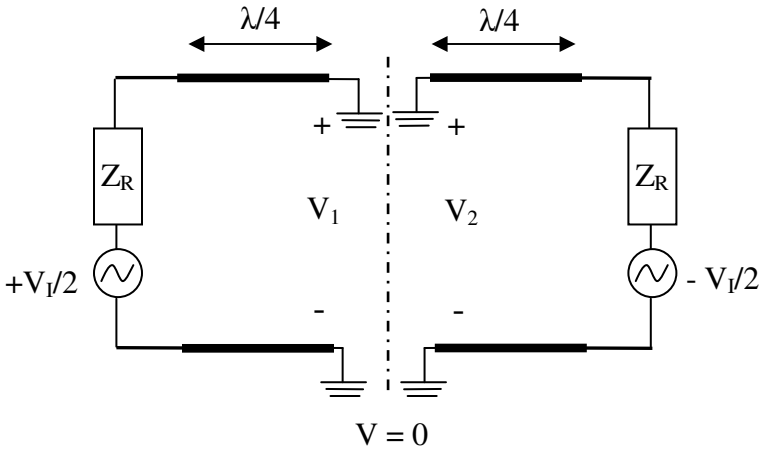


Figure3.7: Odd mode symmetry circuit model

In the Odd mode the plane of symmetry is now a virtual ground. The voltage $V_1$ is equal to $V_I/2$ and $V_2$ is equal $-V_I/2$. We can now extend the plane of symmetry to the matching circuit and the load. Thus the circuit can be completely described using odd mode analysis alone.

### 3.1.2. Odd mode analysis

Odd mode analysis can be extended from the patch to the feed, the matching network, and, the load of the microstrip antenna. We therefore introduce two ports symmetrically at a distance of $l_2$ from the center of the patch as shown in Figure 3.8a. If we consider the width of the feed lines to be very small compared to the length of the rectangular patch, we can

assume that each feed line divides a λ / 4 section of the patch into two parts of length $l_1$ and $l_2$, see Figure 3.8. The patch impedance is then a parallel combination of a short circuit transformed by $l_2$ transmission line length and $Z_R$ transformed by $l_1$ transmission line length, and is represented by $Z_1$. The simplified form of the patch antenna is shown in figure 3.8b.

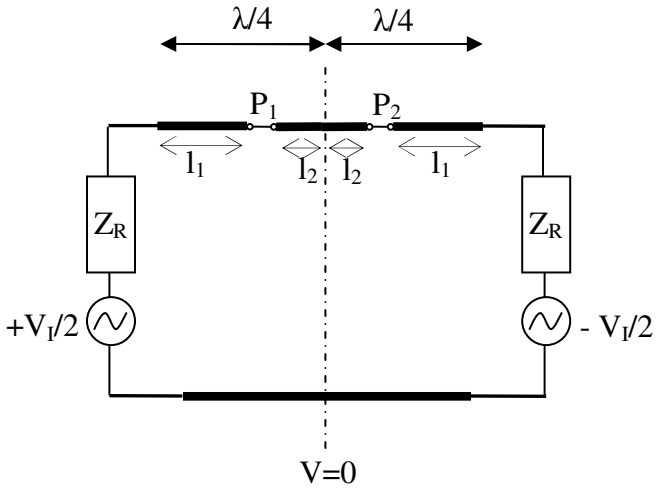


Figure 3.8a: Odd mode circuit symmetry model of microstrip patch antenna with two ports.

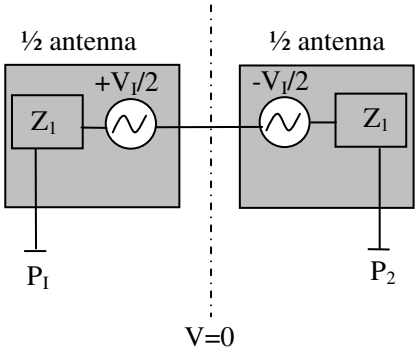


Figure 3.8b: Simplified circuit model of rectangular patch antenna with two ports.

Now, we conceptually divide the antenna with the balanced feed matching network and RFID IC into two halves. The feed lines have a characteristic impedance of $Z_F$ and the shorting stub has a characteristic impedance of $Z_s$. Applying a virtual ground at the line of symmetry the circuit is redrawn as in Figure 3.9. If one views only one half of the circuit

(Figure 3.9) with the radiation impedance, characteristic impedance of the transmission line, line lengths, and the dashed line as a ground, it is apparent that this is a simple, single unbalanced feed microstrip patch with single shorting stub matching circuit as seen in Figure 3.1a. We know that the load impedance is equal to the RFID IC impedance denoted by R - jX. The total antenna impedance must then be equal to its complex conjugate R + jX.

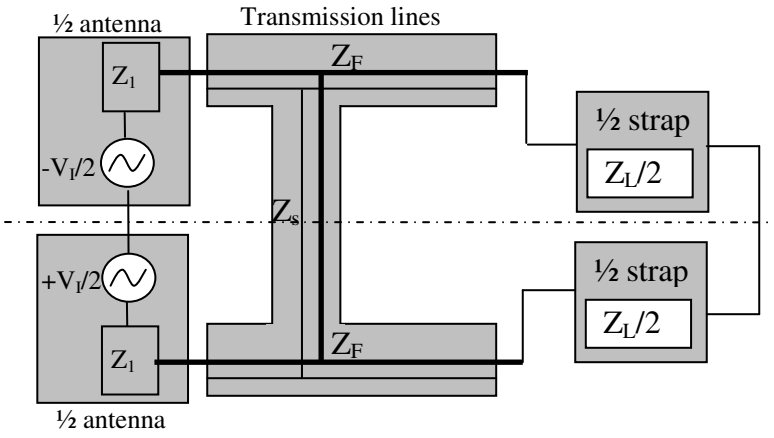


Figure 3.9: Circuit model of microstrip patch antenna with balanced feed matching network.

The ports $P_1$ and $P_2$ are now defined at the end the feed transmission line; the ports are referenced with respect to each other, instead of reference to ground; see Figure 3.10a. The two ports are therefore combined to give one differential port. By symmetry $P_1$ and $P_2$ have equal impedance. It is therefore sufficient to determine the impedance at one port. The total impedance across $P_1$ and $P_2$ is twice the single port impedance. The impedance at $P_1$ is the patch impedance transformed by sections of feed transmission line and a shorting stub.

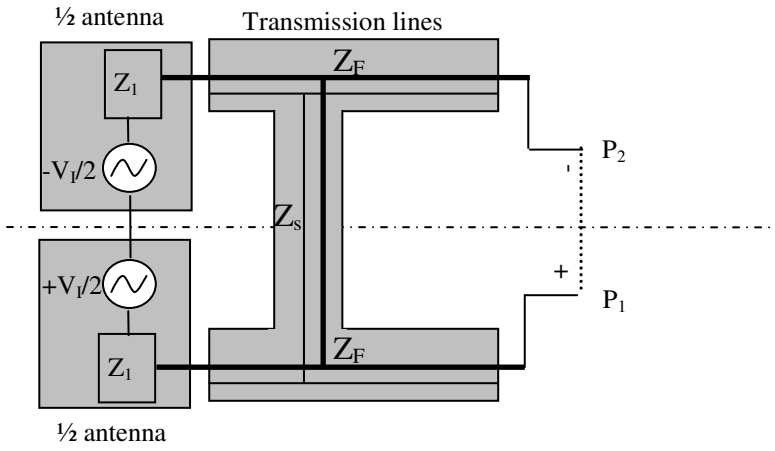


Figure 3.10a: Circuit model of microstrip patch antenna with two ports.

The ports divide a $\lambda / 4$ section of the patch into two sections of lengths $l_1$ and $l_2$, see Figure 3.8a. The impedances $Z_{01}$ and $Z_{02}$ are the input impedances at the end of at $l_1$ and $l_2$ transmission line section with $Z_A$ characteristic impedance. $Z_{01}$ has zero load i.e., it is short circuited and $Z_{02}$ has a load $Z_R$. The impedances can be calculated using transmission line input impedance equations [38] as follows.

$$Z_{01}(x = l_2) = \left( \frac{0 + jZ_A \tan \beta x}{Z_A + j0 \tan \beta x} \right) \tag{3.4}$$

$$Z_{02}(x = l_1) = \left( \frac{Z_r + jZ_A \tan \beta x}{Z_A + jR_r \tan \beta x} \right) \tag{3.5}$$

The impedances $Z_{01}$and $Z_{02}$ are in parallel and hence the total impedance is given by equation 3.6.

$$Z_1 = Z_{01} \parallel Z_{02} \tag{3.6}$$

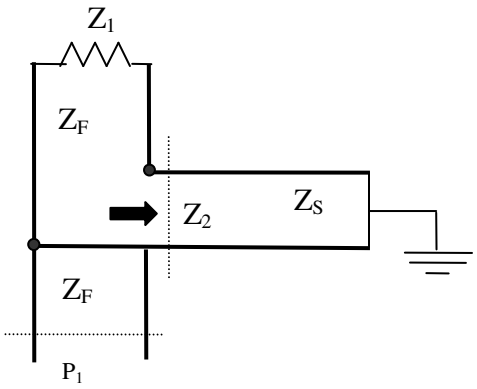


Figure 3.10b: Equivalent circuit model of microstrip patch antenna impedances.

The shunt shorting stub transforms a short circuit load by a section of transmission line length; see Figure 3.10b. The resulting impedance of the stub is purely reactive. Assuming the shorting stub has length of $l_s$ the input impedance $Z_2$ is given by the following equation.

$$Z_2(x = l_s) = \left( \frac{0 + jZ_s \tan \beta x}{Z_s + j0 \tan \beta x} \right) = \boldsymbol{j \tan \beta l_s} \qquad (3.7)$$

The circuit is further simplified as shown in Figure 3.10c.

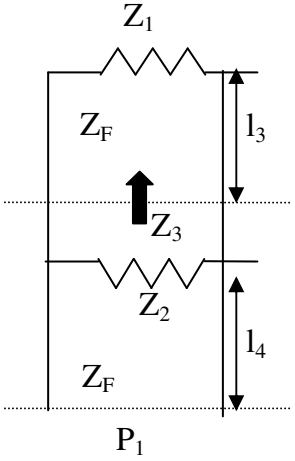


Figure 3.10c: Equivalent circuit model of antenna and shorting stub impedances.

Thus the final impedance at port $P_1$, called the antenna input impedance and denoted by $Z_{in}$ is given by equation 3.8.

$$Z_{in}/2 = Z_F\left(\frac{(Z_2 \parallel Z_3) + jZ_F \tan\beta l_4}{Z_F + j(Z_2 \parallel Z_3)\tan\beta l_4}\right) \quad (3.8)$$

Where $Z_3$ is given by equation 3.9.

$$Z_3 = Z_F\left(\frac{Z_1 + jZ_F \tan\beta l_3}{Z_F + jZ_1 \tan\beta l_3}\right) \quad (3.9)$$

With known values for $Z_A$, $Z_s$, $Z_F$ and $Z_R$ we can determine the lengths of transmission line lengths $l_1$, $l_2$, $l_3$ and $l_4$ required to result in a conjugate match with the RFID IC impedance.

*Cross coupling effect*

Balanced feed matching network design has two feed lines and a shorting stub transmission line that lie on same plane. The coplanar nature of this design, where transmission lines are in proximity of each other causes cross – coupling between them [38]. The effect of cross coupling is predominantly capacitive as shown in Figure 3.10d [38, 39]. The cross coupling capacitance is given by $C_{12}$. Cross coupling between transmission lines causes change in the characteristic impedance of transmission lines and hence the resultant port impedance.

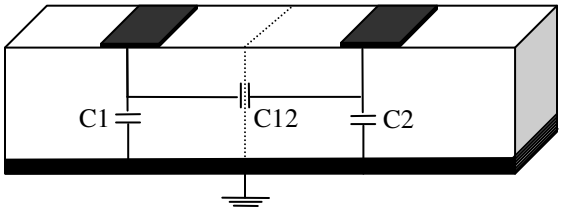


Figure 3.10d: Cross – coupling between coplanar transmission lines [39].

Since these effects are not accounted for in the theoretical odd mode analysis using transmission line equations, the transmission line lengths have to be manually adjusted using simulation tools to achieve the desired impedance match.

## 3.2. Characterization of materials

In the implementation of the balanced feed matching network design for microstrip RFID tags, one of the main considerations is to reduce construction complexity and therefore the cost of the tag. The tag construction is as shown in Figure 3.11. The tag constitutes of a substrate sandwiched between two metal layers; ground plane and antenna plane; the RFID IC is attached to the antenna through a matching network. To attach to an object we remove the bottom liner the pressure sensitive adhesive (PSA) is used to attach the tag to an object. The tag properties are mainly dependent on thickness and dielectric constant of substrate, antenna properties and the RFID IC impedance. Hence the first step in the implementation of the balanced feed matching network design is the characterization of constituent materials. In the following section the procedure for the characterization of substrate and RFID IC is presented.

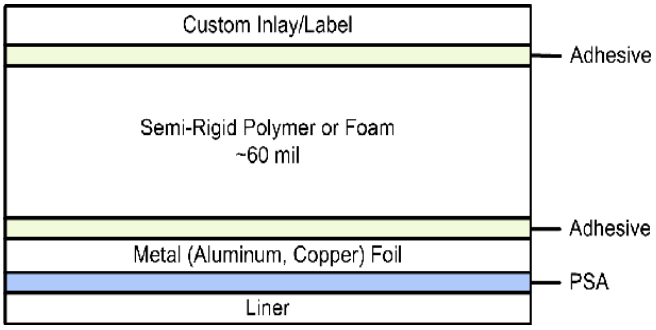


Figure: 3.11 Tag construction.

### 3.2.1. Dielectric of substrate

In order to minimize cost, we chose readily available plastics like high density polyethylene (HDPE) and polypropylene (PP) for substrate material. The dielectric constant ($\varepsilon_r$) is defined

as the ability of a substrate to retain charge [41] and loss tangent (tanδ) is the power lost from the patch antenna due to heating up of the substrate [42]. We use experimental methods to determine the $\varepsilon_r$ and tan δ of these materials. For a known value of $\varepsilon_r$ and dielectric thickness we can calculated the effective dielectric constant ($\varepsilon_{eff}$) and thus the length of resonance of a microstrip patch of given width [32]. This principle is used to determine the $\varepsilon_r$ of HDPE and PP.

We measured the material thickness using a vernier calipers and found it to be 62 mils for both HDPE and PP. The experimental design is based on the initial assumed values for $\varepsilon_r$ and tan δ of the materials. A test resonant patch is designed based on these assumptions. It is experimentally tested and the measured resonant frequency is then used to estimate the actual value of $\varepsilon_r$ and tanδ.

*Assumptions and Initial design*

The test resonant patch is designed assuming, both materials have an $\varepsilon_r$ of 2.25 and tan δ of 0.001. A microstrip patch antenna that resonates at 882 MHz is designed with the following parameters using Ansoft Designer© simulation software. The effective dielectric constant is given by equation 3.10 [32].

$$\varepsilon_{eff} = \frac{\varepsilon_r + 1}{2} + \frac{\varepsilon_r - 1}{2}\left[1 + 12\frac{h}{W}\right]^{-1/2} \qquad (3.10)$$

Where $h$ = height of substrate and $W$ = width of the patch. The height of dielectric is measured to be 62mils = 1.57mm, if the patch width is 10mm and assuming $\varepsilon_r$ = 2.25. Then $\varepsilon_{eff}$ is = 1.7334. The effective wavelength is given by equation 3.11 where $\lambda_0$ is free space wavelength for the given frequency.

$$\lambda_{eff} = \frac{\lambda_0}{\sqrt{\varepsilon_{eff}}} = 25.6625cms \qquad (3.11)$$

The resonant length of the patch at 882 MHz is equal to $\lambda_{eff}$ * 0.49 = 12.5746cm [32].

A single 50Ω microstripline feed is connected to the patch. The antenna impedance at resonance is matched to 50Ω by adjusting the position of the microstripline feed. Adding a length of transmission line to the patch as a feed line changes its resonant frequency therefore the length is patch is tuned to make it resonate at the desired frequency; the effect on feed line length on resonant frequency is further investigated in Section 3.3.3. SMA connector is soldered to the 50Ω line and the refection coefficient at port 1 of the network analyzer is measured.

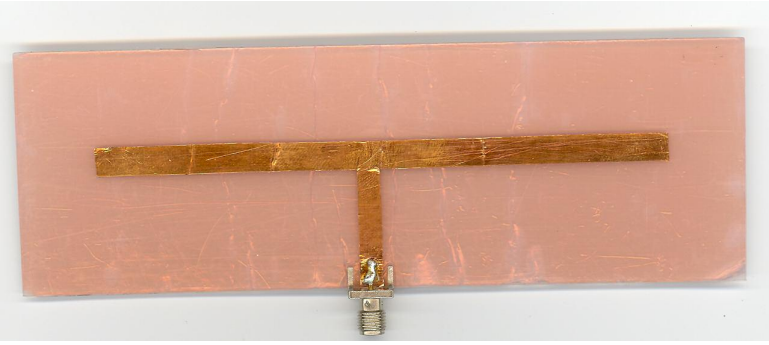

Figure 3.12a: Experimental patch design to determine substrate properties.

*Measurement and results*

The resonant test board is connected to a network analyzer through a 50Ω cable attached to the SMA connector. The $S_{11}$ is measured from 700 to 1000 GHz. If our assumed values are accurate the network analyzer results will coincide with the simulated results. The following graph (Figure 3.12b) shows the network analyzer results for HDPE and PP respectively compared with the simulated $S_{11}$.

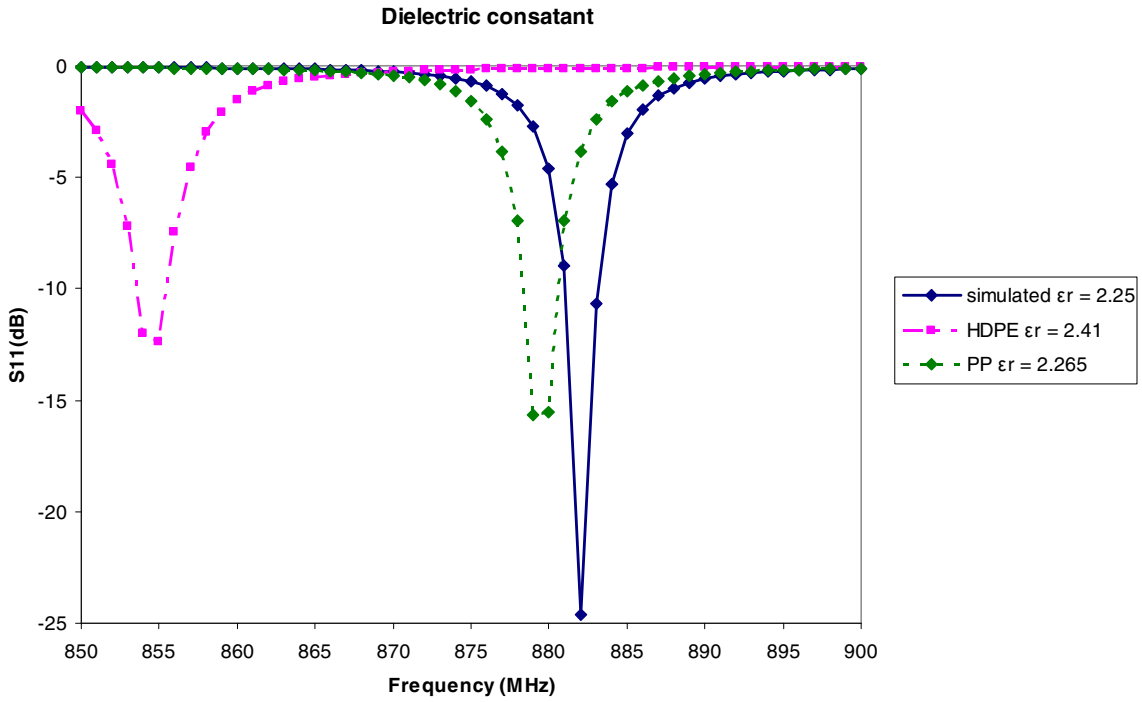


Figure 3.12b: Refection coefficient vs. frequency for simulated and measured values of $\varepsilon_r$.

We observe that for both HDPE and PP the resonant frequency is below 882 MHz at 855 and 879 MHz respectively. Therefore HDPE and PP have $\varepsilon_r > 2.25$. For PP however, the difference in the resonant frequency is approximately 4MHz, the actual $\varepsilon_r$ is close to the assumed value and for accurate estimation a very small step size is chosen.

We re-ran the simulations on the test boards for $2.25 < \varepsilon_r < 2.5$, in steps of 0.01. The results show that the patch resonates at lower frequencies as $\varepsilon_r$ increases. In the next step the loss tangent is adjusted to obtain a reasonable agreement in the simulated and measured impedance values. The properties of HDPE and PP, after the values of $\varepsilon_r$ loss tangent were adjusted to match the measured results are summarized in Table 3.1.

| Material | Simulated resonance | Measured resonance | Measured $\varepsilon_r$ | Measured tanδ |
|---|---|---|---|---|
| **HDPE** | 882 MHz | 855 MHz | **2.41** | **0.0035** |
| **PP** | 882 MHz | 879 MHz | **2.265** | **0.0012** |

Table 3.1: Measured substrate properties.

### 3.2.2. RFID IC impedance

For maximum power transfer between the tag antenna and the RFID IC, the tag antenna impedance must be the complex conjugate of the RFID IC impedance. The RFID IC impedance can be modeled as shown in Figure 3.13a. It is a large resistor of in parallel with a small valued capacitor. If we assume the resistor is 2 KΩ and the capacitor is 1.2 pF then, at the deign frequency of 915 MHz the total IC impedance is given by $Z_{IC.}$

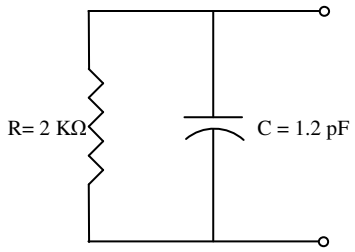


Figure 3.13a: Circuit model of the RFID IC impedance.

$$Z_{IC} = R \amalg X_c \tag{3.12}$$

Where
$$X_c = \frac{-j}{2\pi f_r C} = \frac{-j}{2\pi * 915 * 10^6 * 1.2 * 10^{-12}} = -j173 \tag{3.13}$$

$$\begin{aligned} \therefore Z_{IC} &= 2K\Omega \amalg -j173 \\ &= 14.8 - j171 \end{aligned} \tag{3.14}$$

Depending on the type of IC technology used the RFID IC impedance varies, some of the standard chip impedances according to [39, 40] are given below.

EPC Class 1 Gen 1 at 915 MHz: 6.7 – j197.4Ω.

EPC Class 1 Gen 1 at 868 MHz: 7.4 – j218 Ω.

EPC Class 1 Gen 2 at 915 MHz: 33 – j112 Ω.

EPC Class 1 Gen 2 at 866 MHz: 36 – j117 Ω.

The method used to attach the RFID IC can however change its impedance considerably. There are two types IC of attachment to the tag. Chip attach, allows the RFID IC to be directly connected to the antenna; the antenna impedance is then designed to be a complex conjugate of $Z_{IC.}$ On the other hand, the RFID IC is connected to two mounting pads with a thin superstrate, this is called a strap; see Figure 3.13b. The strap is then attached to the antenna by conductive epoxy. In this process the RFID IC impedance changes due to the epoxy and the strap dimensions. Direct chip attach requires high degree of precision and cannot be done manually. Instead we use strap attach that can be done manually but requires estimation of the strap impedance when attached with conductive epoxy.


Figure 3.13b: RFID IC in strap form, with reference scale.

*Experimental setup*

The RFID IC impedance is measured using a network analyzer, by mounting it on a test board designed and calibrated to take into account the effects of conductive epoxy. The test board is designed on a FR4 substrate with $\varepsilon_r = 4.3$. The signal trace (i.e. the microstrip line

that is connected to the signal pin of the SMA connector) length is kept electrically very short at less than 8mm i.e. less than $\lambda_{eff}$/10 and has a characteristic impedance of 50Ω. The ground pour (i.e. the copper around the signal line) is connected to the actual ground plane by vias. A separation of 2mm is given between the signal trace and the ground pour. Two mounting pads for the RFID IC, one form the signal line and the other from a transmission line connected to ground (using a via) are used to mount the device under test i.e. the RFID IC.

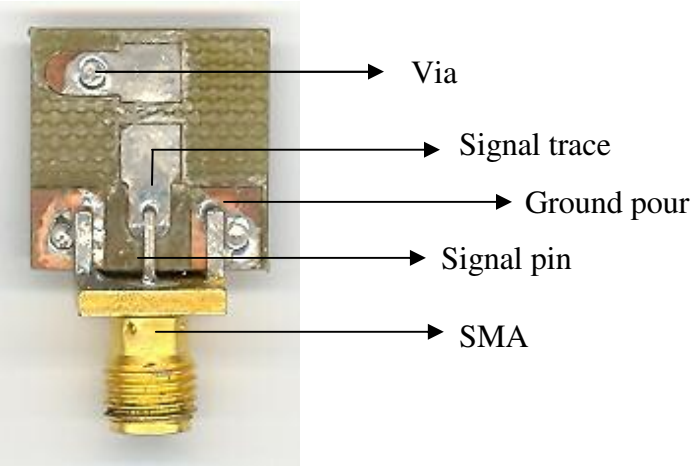


Figure 3.14a: RFID strap impedance measurement board.

The impedance of the RFID IC is measured by mounting it on the test board and testing it with a network analyzer. Before the measurement however the network analyzer is calibrated. The standard 3 point calibration using a perfect short, open and 50Ω load is performed in order to remove any system inaccuracies including connecting cable losses and imperfections. This procedure is rigorously followed when testing RF boards. Using this calibration technique allows us to characterize the complete board along with it components. In finding the impedance of the RFID IC however the test board characteristics must be not

affect the measured IC impedance. Therefore a calibration method that allows the board imperfections to be incorporated in the calibration itself is used.

Network analyzer is calibrated using a three point method, however the points are generated on the test board itself instead of using the perfect open, short, and, load. The open circuit impedance is give by the test boards without any load across it mounting pads. A copper strip connected across the mounting pads gives a short circuit. A 50Ω resistor connect with conductive silver epoxy is used for a standard load. The calibration is verified by placing resistors of know value across the mounts and comparing the actual value with that measured on the network analyzer. All resistor values were measured to be within +/- 1% of the actual value. The RFID IC is now placed on the test board and its impedance between 860 to 960 MHz is measured.

*Measurement and results*

Two types of RFID straps i.e. EPC Class I Gen 1 and EPC Class I Gen 2 [22] are characterized using the above method. The IC technology used in the two types of straps is significantly different and therefore the measured impedances are also dissimilar. Straps of each type were tested by manually applying a silver epoxy on the test board mount pads and placing the strap on it. A small amount of epoxy is used inorder to prevent the strap from being short circuited due to the spreading of the epoxy. The results for each type are averaged. Shown below are the averaged impedance (real and imaginary) values from 860 to 960 MHz.

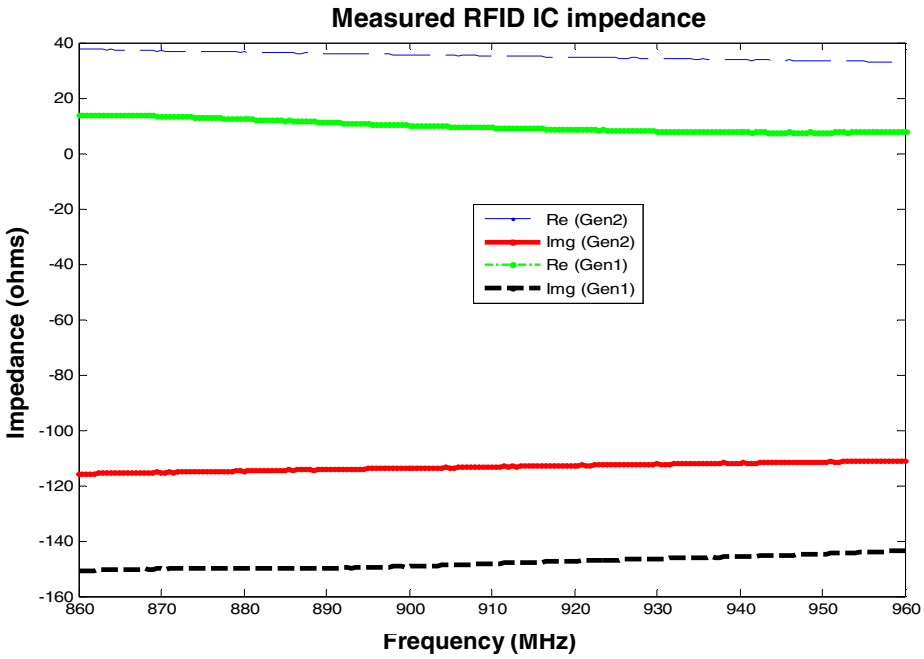


Figure 3.14b: Measured RFID IC impedance for EPC class 1 Gen 1 and Gen2.

The $Z_{IC}$ is therefore taken to be 10 - j150 Ω for EPC class I Gen 1 straps and 35 - j110 Ω for EPC class I Gen 2 straps.

### 3.3. Design parameters

In the following sections we will examine the design parameters involved in the construction of a microstrip antenna with balanced feed matching network and how they affect antenna performance using simulated as well as experimental results. The design parameters are divided into two categories. Antenna parameters include substrate properties, length and width of the rectangular patch and the microstrip feed transmission line characteristics; matching network parameters discuss shorting stub characteristics and its position with respect to the patch antenna.

It is necessary at this point to note that all the design parameters are inter-related, as we will see in the coming sections and not all their effects on the antenna performance are fully understood. In the last two sub-sections we present an analysis of the effect of transmission line length and finite ground plane on resonant frequency using simulated and measured results.

### 3.3.1. Antenna parameters

A microstrip patch antenna is constructed by sandwiching a layer of dielectric between two conducting planes, the ground and the antenna. The antenna itself is made of a patch with feed. The schematic representation of a rectangular patch antenna with balanced feed transmission lines is shown below with parameters designated as detailed in Table 3.2

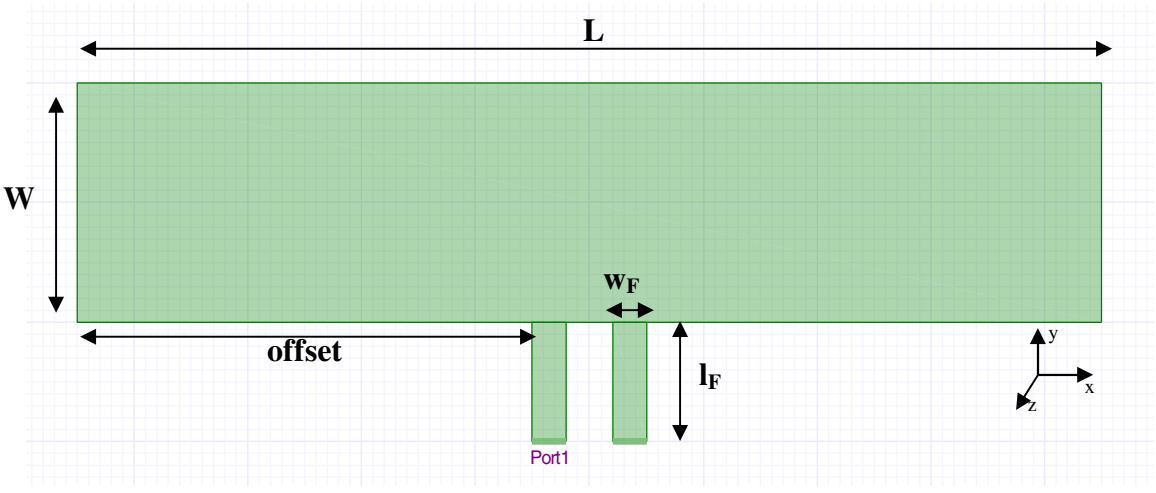


Figure 3.15: Rectangular patch antenna with balanced feed transmission lines - top view.

| Parameter | Description | Parameter | Description |
|---|---|---|---|
| L | Length of rectangular patch | offset | Distance of the feed line from the radiating edge |
| W | Width of rectangular patch | $l_F$ | Length of balanced feed transmission line |
| $w_F$ | Width of balanced feed transmission line | tanδ | Loss tangent of substrate |
| $\varepsilon_r$ | Dielectric of substrate | h | Height of substrate |

Table 3.2: Notations used for antenna parameters.

The first step in designing a microstrip antenna is the selection of a substrate with suitable $\varepsilon_r$ and height. The value $\varepsilon_r$ has both real and imaginary parts.

$$\varepsilon_r = \varepsilon_{\mathrm{Re}} + j\varepsilon_{\mathrm{Im}} \tag{3.15}$$

The real part accounts for charge retention, while the imaginary part accounts for the loss in the medium. The substrate dielectric constant determines the resonant frequency of the patch. Resonant length is inversely proportional to the square root of $\varepsilon_{r;}$ see equation 3.11. Thus higher dielectric constants are preferred as they result in smaller resonant lengths. But substrates with high dielectric constants have larger losses [32]. The $\varepsilon_r$ determines the fringing fields at the patch periphery, low values of $\varepsilon_r$ increases the fringing fields and thus the radiated power [32].

If we consider that the patch and the ground plane act as two conducting plates with a dielectric medium between them we can view the microstrip antenna as a capacitor. The capacitance due to dielectric is given by equation 3.16.

$$C = \varepsilon_r \varepsilon_0 \frac{A}{d} \tag{3.16}$$

Where $\varepsilon_r$ is the relative dielectric constant, $\varepsilon_0$ is dielectric constant of free space, 'd ' is the separation between the conducting plates and is equal to the dielectric thickness h. Since the imaginary part of $\varepsilon_r$ is accounted for in the loss tangent we consider the dielectric constant for all practical purposes to be as shown.

$$\varepsilon_{Re} = \varepsilon_r \tag{3.17}$$

'A' is the area of the conductor plates and 'd' is the separation between them. The antenna and the ground planes act as conducting plates. The Q-factor of the antenna and therefore the antenna bandwidth depend on $\varepsilon_r$ and h of substrate [32]. At higher $\varepsilon_r$ the capacitance between the two conducting planes is larger and so is the Q-factor of the antenna.

Dielectric loss (due to the substrate) along with conductor/ohmic loss (due to finite conductivity, skin effect and roughness of metal conductors) and radiation loss constitute the losses in a system [32, 42, 43]. The total Q-factor of an antenna is dependent on all the above losses. $Q_{dielectric\ loss}$ is defined in equation 3.16 [43, 32]. High value of loss tangent results in poor radiation efficiency and hence low peak gain, Q-factor is inversely related to loss tangent [32] and hence decreases. The 3dB bandwidth defined as the difference between the frequencies within which gain of the antenna power drops by 3dB from its peak value. As tan δ increases the 3 dB bandwidth also increases as bandwidth is inversely proportional to Q-factor of the antenna [38].

$$\tan\delta = -\frac{\varepsilon_{\mathrm{Im}}}{\varepsilon_{\mathrm{Re}}} \qquad \text{and} \qquad Q_{dielectric\ loss} = \frac{1}{\tan\delta} \tag{3.16}$$

After the selection of material based on $\varepsilon_r$ and loss tangent, the only tunable parameter in the substrate is the substrate thickness h. The ratio of width of patch to the dielectric height W/h for a given $\varepsilon_r$ determines the antenna Q-factor and the radiation resistance [32]. From equation 3.16 we know that the capacitance due to dielectric depends on the dielectric thickness. For a given $\varepsilon_r$ as W/h increases (i.e., height decreases) the radiation resistance increases and bandwidth decreases. Hence thicker substrates are preferred as they increase radiated power, reduce conductor loss and improve bandwidth [32]. However using thicker substrates will also increase weight, dielectric loss and surface wave loss [44]. Most high dielectric materials also have large loss tangents. Thus for given frequency of operation, substrates with higher values for $\varepsilon_r$ result in low gain, large 3dB bandwidth and smaller size antennas whereas, low value dielectric materials give large peak gain narrow 3dB bandwidth and require a larger form-factor. Therefore a careful selection of substrate is critical in determining the form-factor and the Q-factor of the antenna. We chose HDPE as the substrate for our designs in this section as it is low cost, easy to work with, and showed consistent substrate properties. PP samples were found to have inconsistent properties. HDPE also has greater tan $\delta$ that gives better bandwidth compared to PP, though peak performance is slightly reduced.

A rectangular patch offers less complexity in terms geometry. On a substrate of known $\varepsilon_r$ and height h the patch can be simply defined by L x W, where L is the resonant length defined along the x-axis and W is the width along the y-axis. While operating in $TM_{10}$ mode

the electric and magnetic fields vary along the length while remaining constant along the width. Thus the length L is critical in determining the frequency of resonance. The fringing fields the radiating ends of the rectangular patch cause radiation The patch impedance (see equations 3.4 to 3.6) is determined by the selection of feed point position along the patch. The microstrip feed transmission line width and length transform the actual patch impedance as given by equations 3.8 and 3.9 and have to selected appropriately to result in a conjugate match with the RFID IC.

A rectangular patch is essentially a microstrip a transmission line; hence the width of the patch determines its characteristic impedance and the fudge factor [32, 36]. It is used to for calculate the effective patch length [32, 36]. Larger patch width implies small characteristic impedance, reduced radiation resistance, and, increased aperture. It therefore increases radiated power, bandwidth and radiation efficiency.

At a given frequency of resonance and $\varepsilon_r$ of dielectric the length L is almost always chosen to be odd multiples of half the effective wavelength (given in equation 3.11) long to make the patch radiate efficiently. To operate in the fundamental $TM_{10}$ mode the length L is taken to be a little less than ½ the effective wavelength in order to account for a fraction of the fringing fields that lie outside the physical dimensions L x W [36]. The electrical length of the antenna which is different from its physical length L is discussed in Section 3.3.3.

The position of the feed transmission line with respect to the patch determines the patch impedance and hence the total antenna input impedance. The distance from the radiating

edge to the feed point is defined as the offset. As the offset increases the feed lines are closer to the virtual ground and the patch impedance is very small, feeding close to the radiating ends increases the patch impedance. Figure 3.16 shows the comparison of input impedance at resonance for different offset values.

The characteristic impedance of the feed plays a vital role is determining the final port impedance. Wider feed lines imply small characteristic impedances. This will result in the reactive component of the antenna input impedance being more capacitive compared to the impedance when narrow feed lines. Narrow transmission lines add inductive reactance to the input impedance. The variation in the port impedance for different feed line widths is shown in Figure 3.17.

Setup: $\varepsilon_r = 4.35$, $\tan\delta = 0.02$, h = 62 mil, L = 90mm, w = 20mm $l_F = 5$mm, $w_F = 3$mm

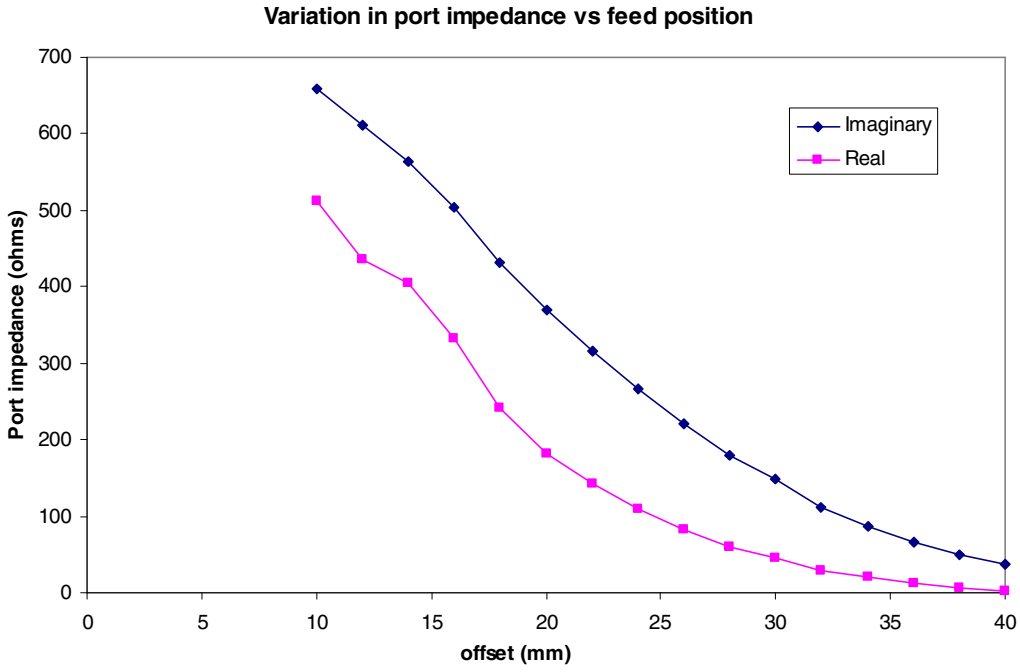


Figure 3.16 : Variation in simulated patch imedance with feed position – offset.

Setup: $\varepsilon_r = 4.35$, $\tan\delta = 0.02$, h =62 mil, L = 90mm, w = 20mm, $l_F$ = 20mm, offset = 30mm

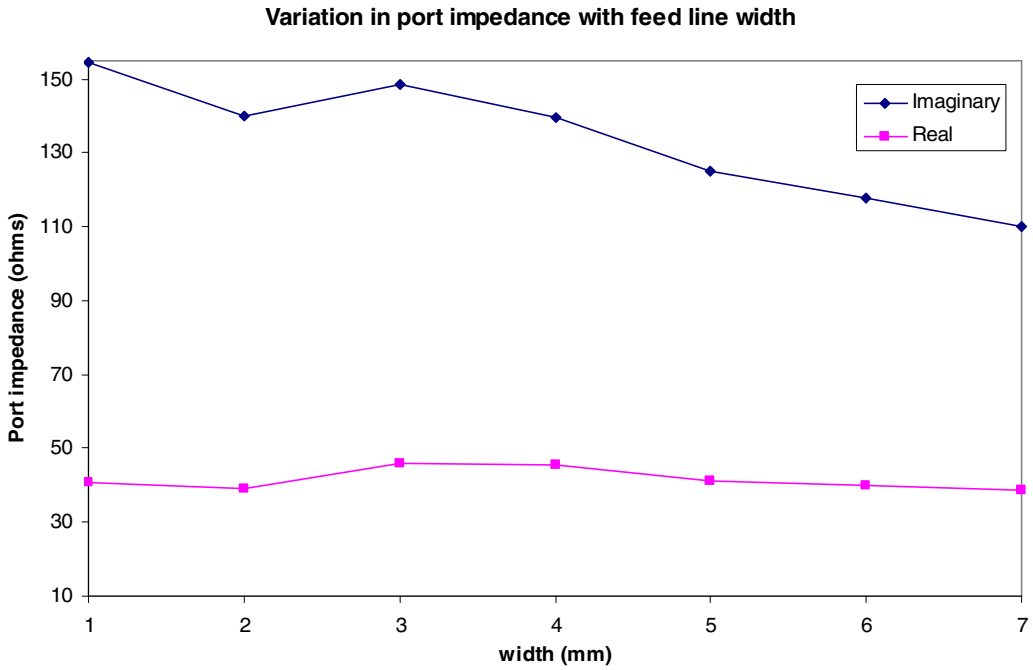


Figure 3.17: Variation in simulated port impedance with feed line width.

The port impedance is affected by adding a length of transmission line to feed the patch. We know that a transmission line transforms the patch impedance by its characteristic impedance and length (refer equations 3.6-3.9). Therefore by lengthening the feed line we will be adding a reactive component to the antenna impedance.

In section 3.2.2 we experimentally found that the RFID IC impedance is largely capacitive; therefore the conjugate port impedance must be inductive. We therefore use considerable lengths of narrow feed line connected close to the virtual ground to achieve low resistive and highly reactive input impedance. However the balanced feed design where, the feed lines and the resonant patch are coplanar, shows variation in the resonant frequency due to change in the feed line parameters. This is because of the change in the electrical length of the antenna; this effect is discussed in detail in the next section.

### 3.3.2. Effect of feed line parameters on resonant frequency

Microstrip antennas have a narrow bandwidth and length of the antenna is critical in determining the resonant frequency. We have seen that to operate in the fundamental $TM_{10}$ mode the length L the antenna is nearly be $0.49^* \lambda_{eff}$ [36], therefore, at lower frequencies the effective wavelength is longer and hence the antenna length. In a balanced feed design however, the total electrical antenna length is different from the physical patch length and depends on the patch width, geometry, and, dielectric constant of substrate. By adding a feed transmission line to the patch, we change the width of the patch at some places and consequently its electrical length. The electrical length determines the resonant frequency.

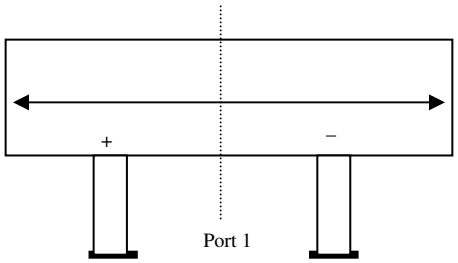


Figure 3.18: Total electrical length of a balanced feed microstrip antenna.

Therefore, changing any of the following offset, length, or width of the feed line; will change the effective electrical length of the antenna. Increasing offset in addition to reducing input port impedance also reduces the electrical length making the antenna resonate at higher frequency. Similarly lengthening the feed line adds reactive impedance and also increases the total electrical length of the antenna thus making it resonate at a lower frequency. These effects are illustrated in the following simulation results.

Setup: $\varepsilon_r = 4.35$, $\tan\delta = 0.02$, h = 62 mil, L = 90mm, w = 20mm, $w_F = 3$mm

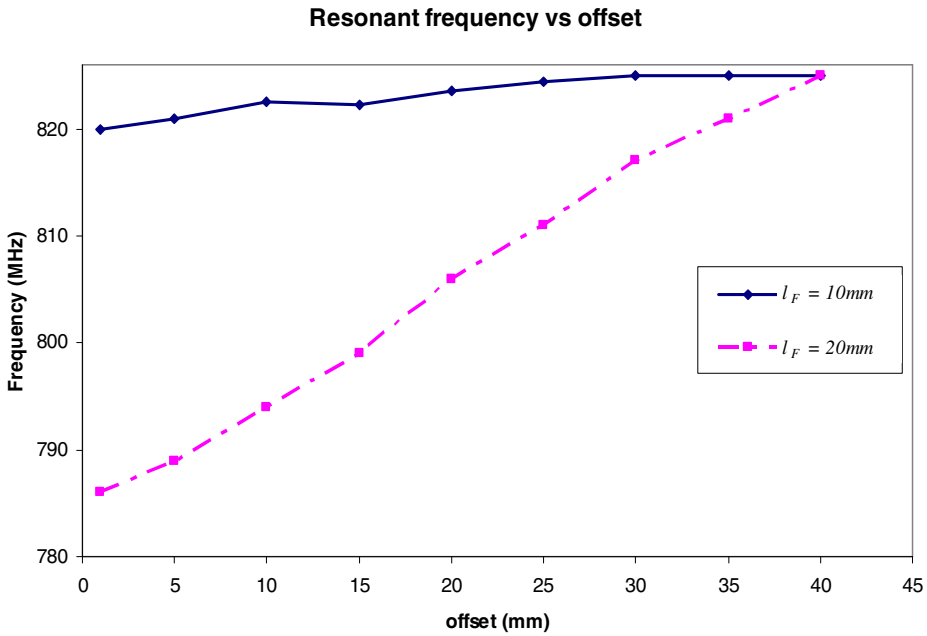


Figure 3.19a: Change in simulated resonant frequency with offset for different feed line lengths.

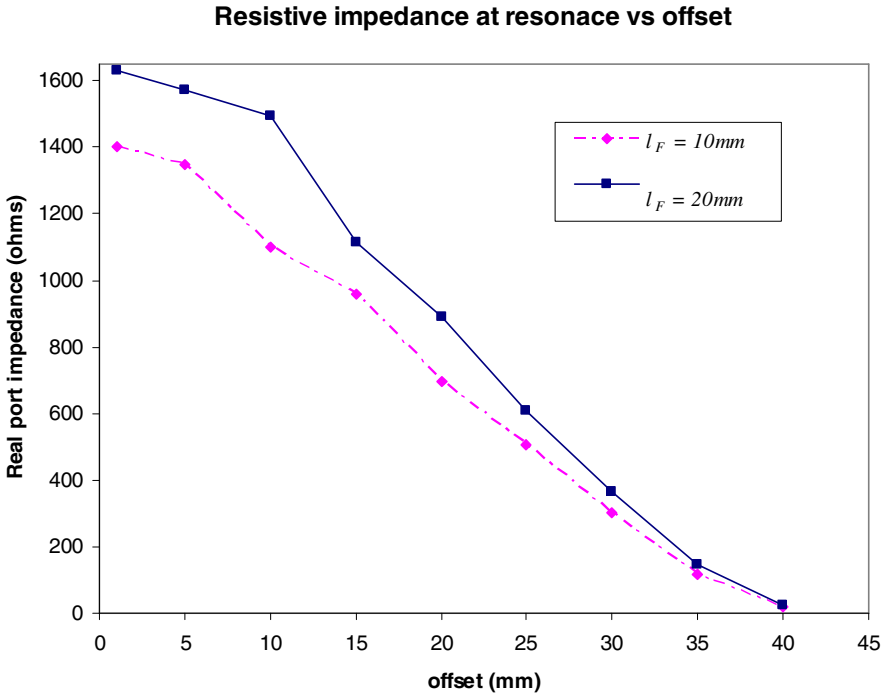


Figure 3.19b: Change in simulated resistive input impedance with offset for different feed line lengths.

We simulated a microstrip patch with the above parameters and noted the variation in the resonant frequency for different values of offset and feed line length. It is observed that for longer lengths of $l_F$ (i.e., $l_F$ = 20mm,) the variation in the resonant frequency is greater than when $l_F$ is smaller (i.e., $l_F$ = 10mm,). Similarly the input impedance varies from 1650 to 24 Ω at $l_F$ = 20mm, with the offset, whereas at $l_F$ = 10mm, the impedance varies between 1400 to 24Ω. As the balanced feed technique has twofold effect on the antenna performance, some amount of manual fine tuning is necessary to obtain the impedance match at the desired frequency. Also the feed transmission line length alone is insufficient to provide the required reactive port impedance; we therefore use shorting stubs.

### 3.3.3. Matching network parameters

The purpose of a matching network is to provide impedance matching between the output port of the source and the input port of the destination [38]. Some of the commonly used matching network designs like quarterwave sections and multi-section transformers are effective in matching purely resistive loads; shorting stubs can be used to match reactive loads [38]. Since the RFID IC impedance is highly capacitive in nature the conjugate match in predominantly inductive. In this case shorting stubs are used to add reactive impedance rather than cancel it.

In a microstrip antenna, at resonance, the resistive impedance peaks while the reactive impedance goes to zero. For thin substrates the resistive impedance at resonance is much greater than reactive impedance [19]. The feed point is chosen such that the resistive impedance is close to the value required to match *15 - j150*. Placing shunt stub to the feed

line will transform the patch impedance by adding a reactive component in parallel to the patch impedance. The circuit analysis of the antenna with a shorting stub was discussed in section 3.3.1. Figure 3.20 shows the variation in the reactive port impedance with and without a shorting stub. When a shorting stub is used, it flattens (reduces difference between the maximum and minimum impedance values) the reactive impedance at resonance, maintaining a nearly constant value.

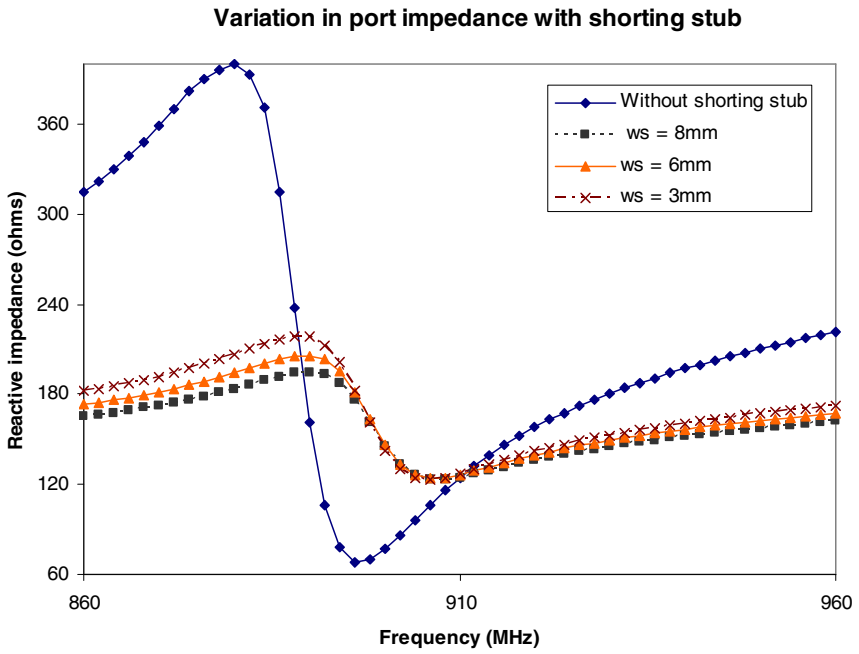


Figure 3.20a: Variation in simulated input port impedance with and without shorting stub.

The length ($l_s$) and width ($w_s$) of the shorting stub determine the degree of flatness that can be achieved.

Though the stub itself adds a purely reactive component to the total impedance, its placement on the feed line scales the resistive impedance of the patch (see Equation 3.7, 3.8). Therefore in addition to flattening the reactive impedance the shorting stub also reduces the resistive

impedance considerably allowing us to connect the feed lines farther way from the virtual ground.

### 3.3.4. Effect of finite ground plane

We use Ansoft Designer software tool to simulate microstrip antenna designs. Ansoft Designer assumes that the antenna plane is backed by an infinite substrate and ground plane. In reality the infinite ground and substrate is replaced by finite ones. A finite ground plane and substrate affect the radiation pattern and resonant frequency of a patch antenna [32]. In the transmission line model of microstrip antennas the radiation pattern is calculated based on the two-slot model [32]. For a patch radiating in the $TM_{10}$ mode a two slots placed along the radiating edges are used to model the antenna. The effect of finite ground plane and substrate are modeled by placing slots at a distance of 'kh' from the ground plane, where k is as defined in equation 3.19 [32] and h is the substrate thickness. Multiplying the resulting factors with the E-plane pattern [32] will account for the effect of ground and substrate.

$$k = k_0\sqrt{\varepsilon_r} \tag{3.19}$$

Where $k_0$ is the free space wave number. However the radiation pattern of the antenna is not taken into consideration and therefore not studied in this thesis.

The speed of propagation of electromagnetic waves through the antenna, and the resulting fringing fields determine the resonant frequency of the antenna. If the ground plane and substrate end at the patch boundary the more fringing fields will lie in free space (i.e. a lower dielectric than the substrate) causing the patch to resonate lower than with infinite substrate and ground planes. We experimentally analyzed the variation in resonant frequency with the size of ground plane. A model assuming infinite substrate and ground planes was simulated.

Measurement prototypes with different sizes of extended ground were fabricated and tested on a network analyzer. The design principle used is same as described in Section 3.2.1. Figure 3.20b shows the measured results. As expected the simulated resonant frequency is lowest at 840 MHz, which is closely approximated by an extended ground plane of 150 mm. As the ground dimensions are reduced the resonant frequency is increases.

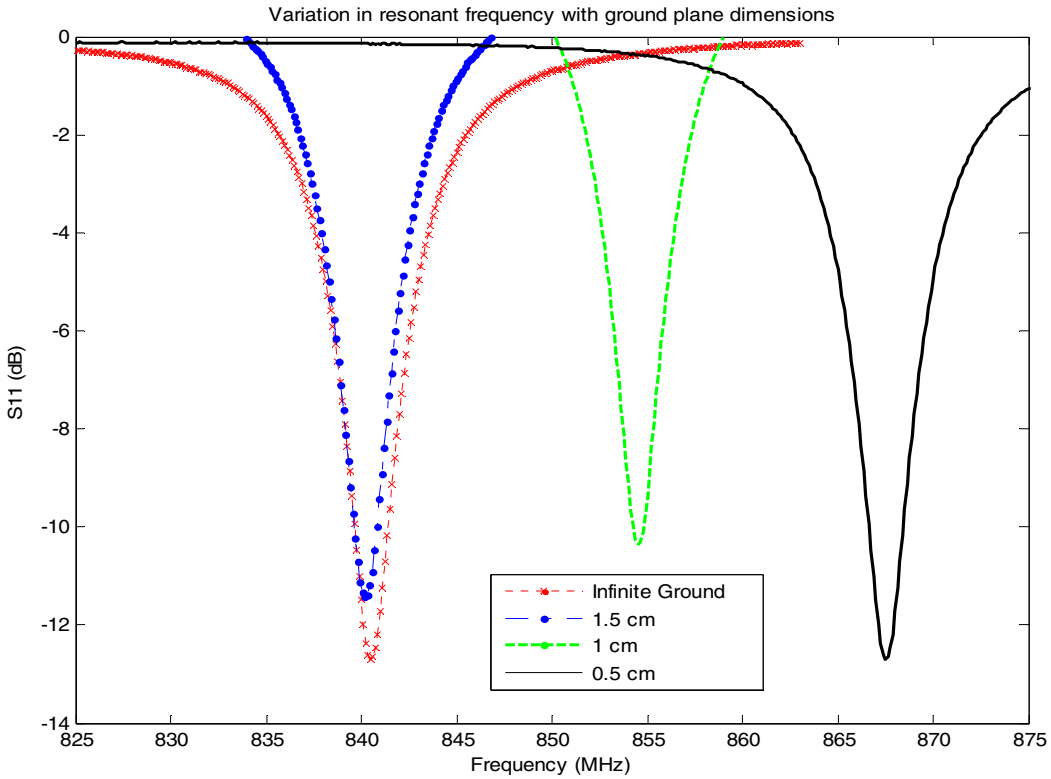


Fig 3.20b: Variation is measured resonant frquency with different finite ground plane extensions.

Based on the above analyses the initial parameters for the microstrip patch antenna with balanced feed are selected. Table 3.3 shows the values.

| Parameter | Value (units) | Parameter | Value (units) |
|---|---|---|---|
| $\varepsilon_r$ | 2.41 | $l_F$ | 10 mm |
| tanδ | 0.0035 | $w_F$ | 2 mm |
| h | 62 mils | offset | ***L/2.5*** mm |
| L | 106.6 mm | $w_s$ | 2 mm |
| W | 35 mm | $l_s$ | 30 mm |
| Extended ground plane | 1.5 cm | | |

Table 3.3: Initial design parameter values for microstrip antenna with balanced feed.

The microstrip patch antenna with balanced feed is implemented with the above parameters. Extensive simulations are used to refine the parameter values in order to achieve the design goals, which are also described in the next section. The following section details the implementation and optimization procedure along simulated results. A discussion of the issues associated with the final design is also presented.

## 3.4. Design Evolution

The design goals for the microstrip patch RFID antenna with balanced feed mechanism implemented in this section are to achieve peak performance at 915 MHz, with a return loss less than -10db throughout the Federal Communications Commission (FCC) bandwidth for RFID operations, keeping small form-factor in consideration. A stage wise implementation procedure is adopted to arrive at the optimum values for the design parameters. The antenna is optimized from the initial dual stub design with a large form factor to the final single stub optimized model through a series of refinements in the parameter values.

### 3.4.1. Single patch antenna with dual stub matching network

The design is based on the parameter values specified in Table 3.3. Ansoft Designer EM simulation tool was used to model the design. Reducing the number of variable parameters allows us to simplify the optimization procedure, therefore for in this design we kept all widths (patch as well as feed and matching stub transmission lines) constant. The first step in implementation was to adjust the patch and feed line lengths to make the antenna resonate at the desired frequency. The widths of the patch and the feed lines remained unaltered through this. Since the offset and resonant lengths are inter-dependent, determining the feed point is non-trivial.

The offset values are varied relative to the length of the patch. Any change in the resonant frequency is compensated by changing the length of the rectangular patch. Offset values are parametrically varied to achieve the correct resistive impedance. We use an EPC Class 1 Gen 1 RFID IC, which has a measured average impedance of 10 - j150. The desire port impedance is hence the conjugate match equal to 10 + j150. Then shorting stubs are used to tune the reactive impedance. Here the stub length and position along the feed line was varied. It was seen that a single shorting stub of the chosen width was insufficient to maintain high reactive input impedance. We therefore used two stubs separated by a distance of 4mm in this design.

Since the placement of shorting stubs reduces the resistive component of the port impedance, the offset is varied to compensate for this reduction. This procedure is repeated several times before we arrive at the final model shown in Figure 3.21. The overall form factor of the tag

antenna is 110mm x 67 mm; the matching network with the balanced feed has dimensions of 37 x 33 mm.

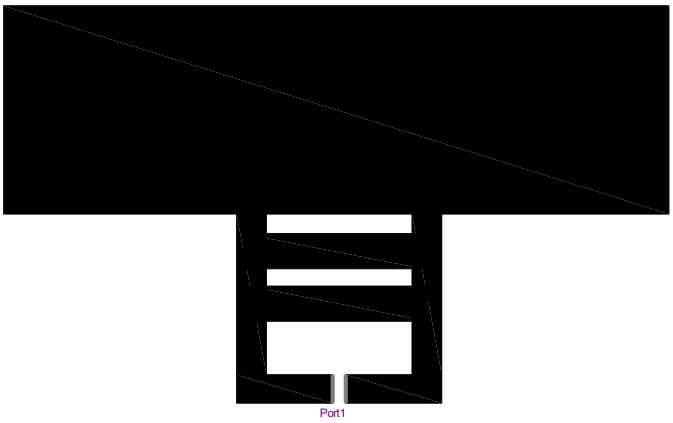


Figure 3.21: Simulation model of the single patch dual stub matching network deign – top view.

The final parameters are detailed in table 3.4. The values that are different from the initial values are highlighted.

| Parameter | Value (units) | Parameter | Value (units) |
|---|---|---|---|
| $\varepsilon_r$ | 2.41 | ***$l_F$*** | ***35 mm*** |
| tanδ | 0.0035 | $w_F$ | 2 mm |
| h | 62 mils | ***offset*** | ***L/2.89*** mm |
| ***L*** | ***110 mm*** | $w_s$ | 2 mm |
| W | 35mm | ***$l_s$*** | ***12.5 mm*** |
| | Extended ground plane | 1.5cm | |

Table 3.4 : Single patch dual stub matching network design values.

The antenna has an impedance bandwidth that exceeds the gain bandwidth. The 3 dB bandwidth measures 8.2 MHz. Peak gain is 0dB and occurs at 917 MHz; see Figures 3.23, 3.24.

### 3.4.2. Single patch antenna with single stub matching network

The single patch antenna with dual stub matching network is a good performer in terms of impedance bandwidth; in this case defined as frequencies between which the return loss is less tan -10dB, and, peak gain. It however, has a large form-factor. Approximately half the total antenna size is due to the double stub matching network. The design optimization is also partial in the sense that all line widths are unaltered from their initial assumed values. In the second stage of design evolution the design parameter values from dual stub design are used as a starting point for designing a new antenna and the design criteria is to minimize the matching network area without affecting the performance. Assuming that the minimum feature size is 1mm, the line widths are also varied, along with other parameters.

The dual stub matching network is replaced by a single shorting stub of 1mm width. The narrow shunt stub has a characteristic impedance of 112Ω on a substrate of HDPE ($\varepsilon_r$ = 2.41). A single narrow stub with large characteristic impedance adds as much reactance as a two lower impedance stubs in parallel. Narrow meandered feed lines also add to the reactive impedance and also reduce the area. Since narrow feed lines will result in greater characteristic impedance as consequently greater input impedance, the offset value is increased and the feed lines are connected closer to the virtual ground. An EPC Class 1 Gen 2 RFID IC with measured average strap impedance 35 - j110 is attached to the antenna,

therefore the target port impedance is the conjugate match given by 35 + j110. The final model and its parameters are given in Figure 3.22 and Table 3.5 respectively. The form-factor of this antenna is 106mm x 41.5mm and the matching network with the feed transmission lines occupies 34mm x 6.5mm of physical space.

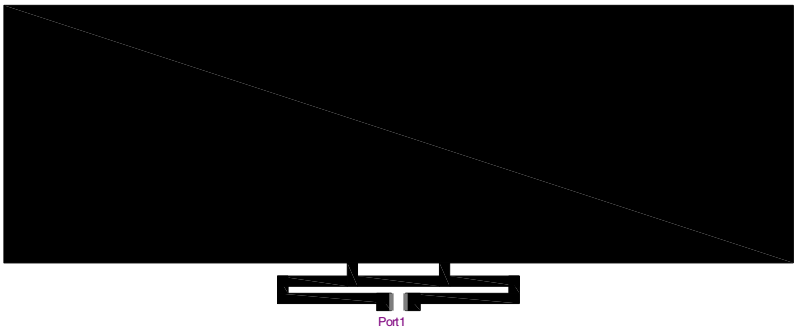


Figure 3.22: Simulation model of the single patch single stub matching network deign – top view.

| Parameter | Value (units) | Parameter | Value (units) |
|---|---|---|---|
| $\varepsilon_r$ | 2.41 | $l_F$ | ***22 mm*** |
| tanδ | 0.0035 | $w_F$ | ***1 mm*** |
| h | 62 mils | ***offset*** | ***L/2.29 mm*** |
| ***L*** | ***106.8 mm*** | $w_s$ | ***1mm*** |
| W | 35mm | $l_s$ | ***5.5 mm*** |
| Extended ground plane | 1.5cm | | |

Table 3.5 : Single patch dual stub matching network design values

The performance comparison between the dual stub and single stub designs is illustrated in Figures 3.23 and 3.24. The single stub antenna has nearly the same performance as the dual stub design in terms of gain; the peak gain is measured to be -1.25dBi at 915MHz. The return loss however, is greater at lower frequencies and smaller at higher frequencies when

matched to EPC class 1 Gen 1 RFID IC. Overall the return loss is well under -10 dB in both cases which is sufficient to enable efficient power transfer. If we exchanged the RFID IC between the designs, even then the return loss is below -10dB, thus making the designs, both EPC Class 1 Gen 1 and EPC Class 1Gen 2 compatible.

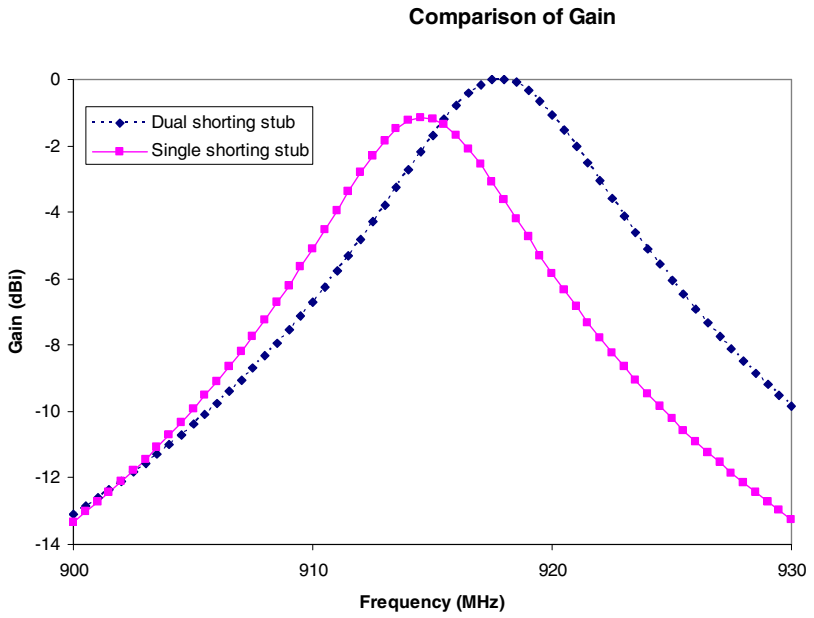


Figure 3.23: Comparision of simulated gains for different matching networks.

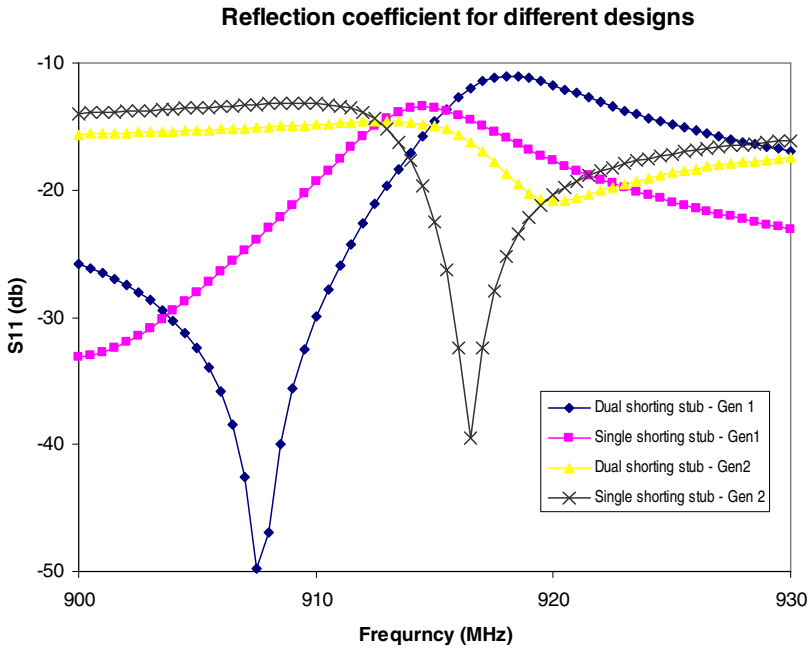


Figure 3.24 : Comparision of simulated reflction coefficient for different matching networks.

### 3.4.3. Optimization and issues

The criteria for optimization of the microstrip RFID antenna performance are

- Maximize power transfer
- Maximum peak performance
- Minimize substrate thickness
- Achieve maximum bandwidth
- Minimize form - factor

The design instantiations presented in this section showed that maximum power transfer occurred in the desired bandwidth irrespective of the RFID IC type chosen. The above designs show that the microstrip RFID tag is gain limited while the return loss is well under -10dB. Further investigation shows that trying to achieve minimum return loss at resonance reduces the peak gain considerably. This is because the antenna gain is related to the resistive component of input impedance as given in equations 3.20 and 3.21 [19].

$$Gain_{(\theta,\phi)} = \frac{\left|rE_{(\theta,\phi)}\right|^2}{30P} \tag{3.20}$$

$|rE|$ is the magnitude of the radiated electric field multiplied by the distance, r and $P$ is the power, in watts which for a single port device is calculate as

$$P = \left|I\right|^2 * \mathrm{Re}\left(Z_{(in)}\right) * \left(1 - \left(S_{11}\right)^2\right) \tag{3.21}$$

Where $Z_{in}$ is the impedance across ports $P_1$ and $P_2$, and $S_{11}$ is the return loss and I is the current at port one taken by default as 1 amp. Therefore matching to very low real impedance (i.e. 10 – 35Ω as the case may be) causes high current densities resulting in larger

Ohmic losses [32] and reduced gain. A tradeoff is therefore established between the port impedance at resonance and the gain. The port impedance is maximized until the threshold of -10dB return loss maintained resulting in good power transfer while maximizing gain. Any further increase in the real value of the port impedance will results in reduced power transfer. The conductive losses are minimized by use of thick copper for the antenna.

The other three criteria are inter-related more difficult to achieve. The microstrip antennas were designed on 62 mil substrate keeping the low profile of the antenna in mind. At this substrate thickness the fractional bandwidth of the antenna is nearly 1%. Minimizing substrate thickness to less than 62 mils will result in severe loss of bandwidth and therefore is avoided. Similarly reducing the form–factor will result in reduce peak performance and bandwidth due to reduced aperture.

The design prototypes presented in this section are sub-optimal realizations in terms of bandwidth and form-factor. In order to achieve optimum performance, techniques such as multi-resonant designs [34] with electromagnetically coupled feeds and more complex patch geometries need to be explored. Preliminary investigation of some of these techniques is presented in chapter 5.

*4.*

# Chapter 4

# Results

The single stub matching network design discussed in chapter 3 is considered to be the optimized planar microstrip antenna design with balanced feed. This design was fabricated in the lab and its performance characteristics were experimentally measured. The prototype validation procedure and measured results are presented in this chapter.

The original intent of this project was to demonstrate that a planar microstrip antenna for RFID applications is possible and show that such a RFID tag will have uniform performance irrespective of the material to which it is attached. The prototype is therefore compared with other commercially available RFID tags near metals and water with read distance as the comparison metric, the results are discussed towards the end of this chapter.

## 4.1. Measured results

The single stub matching network design was simulated using Ansoft Designer, the simulated results were presented in Section 3.4. To validate these results, a prototype was built and a testing procedure was developed.

### 4.1.1. Prototype fabrication

The Ansoft model for the optimize microstrip RFID tag was fabricated in the lab manually. Prototype fabrication is a simple three stage process is easy to implement. Firstly the

substrate is cut to the required size (i.e. antenna dimensions and additional 1.5 cm of extended ground plane). The substrate is now covered with a self adhering copper layer on both sides. The Ansoft Designer model is cut out on one side of the substrate while the other serves as the ground plane. The RFID IC with the strap is then attached to the antenna using conductive silver epoxy. The epoxy used is the same that was used to test the RFID IC impedance. A secondary adhesive layer is applied on the strap to provide mechanical stability to the attachment. Figure 4.1a shows the prototype with a Class 1 Gen 2 RFID IC.

Figure 4.1a: Planar microstrip antenna with balanced feed mechanism – Prototype.

### 4.1.2. Measurement setup and results

Validation and performance measurement of this prototype involves measuring the antenna input impedance and gain over the given bandwidth. Since the antenna is a balanced device it is not possible to directly measure its impedance using a network analyzer. The balanced feed has to be converted into an unbalanced feed using a device called balun. The port impedance can now be directly measured from the balun output using a network analyzer. Alternately, since our design has odd mode symmetry, the input impedance measured at only one of the two balanced feed lines must be equal to ½ the overall antenna impedance; (see

Section 3.1 for details). That is, without using a balun, we can measure the input impedance at the end of one feed transmission line with reference to ground. But feeding the patch with a single balanced feed will change the current distribution on the patch and therefore the far field pattern. The device no longer has only odd mode, an even mode is also present as shown in Figure 4.1b and 4.1c.

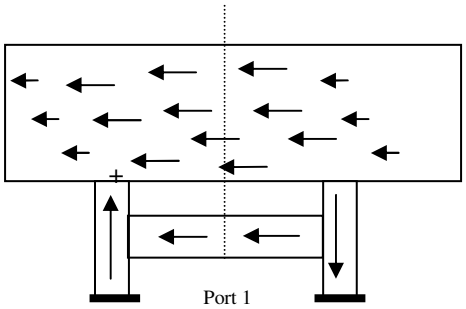


Figure 4.1b: Odd mode current distribution on patch antenna with balanced feed.

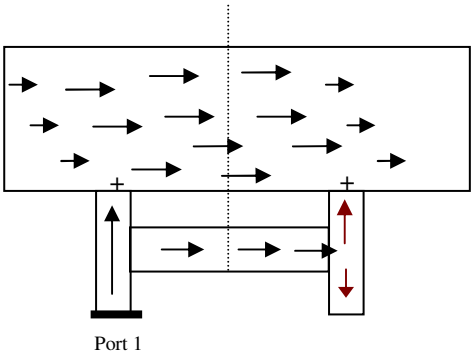


Figure 4.1c: Even mode current distribution on patch antenna with unbalanced feed.

Notice that in Figure 4.1b the balanced feed lines have currents flowing in opposite directions. In Figure 4.1c, only one the feed lines is used to create a port. The current from this feed line through the shorting stub reaches the non – excited feed line. The current here splits in two direction one in the same direction as the current flow in the excited feed line, the other, is in the opposite direction. Thus both even and odd modes exist when unbalanced feed is used.

The even mode, however, does not contribute substantially to the far field radiation at the frequencies in which the device is required to operate. This is shown by simulating the antenna with two ports excited 180 out of phase with each other (i.e., balanced feed) and with a single port excited with reference to ground (i.e., unbalanced feed). The simulated

gains for both cases are compared. We see from Figure 4.1d that though the antenna gain with balanced feed and unbalanced feed are not the same, balanced feed gives greater peak gain and 3dB bandwidth, the difference is not large enough to indicate the preens of an even mode. It is therefore reasonable to assume that though feeding the antenna with a single unbalanced feed creates an even mode its effect on the antenna performance is not significant. We can therefore use a single unbalanced feed to measure the antenna characteristics.

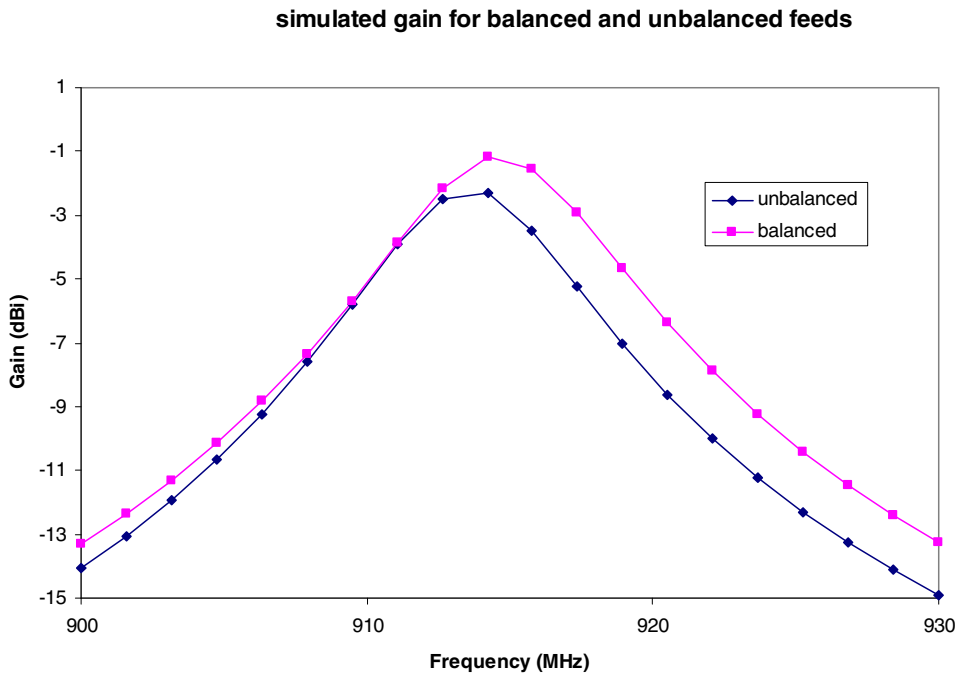


Figure 4.1d: Effect of balanced and unbalanced feed mechanisms on antenna gain.

To measure the antenna input impedance we simulated the design with only one of two feed lines excited with reference to ground. See Figure 4.1e. As expected [Equation 3.8] the resultant impedance was half what we see when the two feed lines are excited 180º out of phase with each other. The strap is removed from the antenna and the signal pin of a SMA connector is now soldered to one end of feed transmission line, the ground pins are

connected to the ground plane. The network analyzer is calibrated with 1 meter long 50Ω cables from 860 to 960 MHz. The microstrip antenna is connected to the network analyzer port through the SMA connector and the return loss at $P_1$ is measured. Figure 4.1e shows the measurement prototype and Figure 4.2 shows the measured and simulated input impedances for a single port excited with reference to ground.

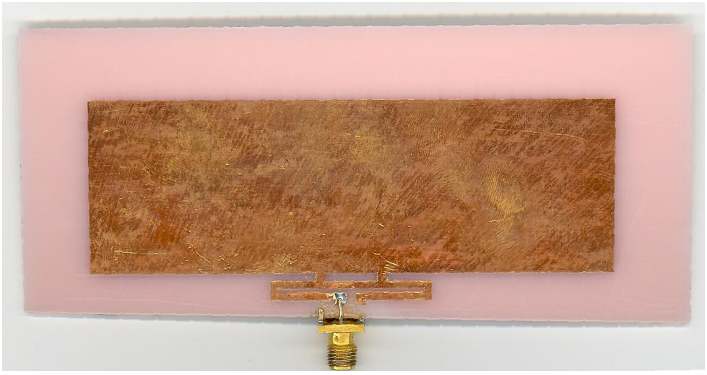

Figure 4.1e: Measurement prototype with single unbalanced feed connected to a SMA connector.

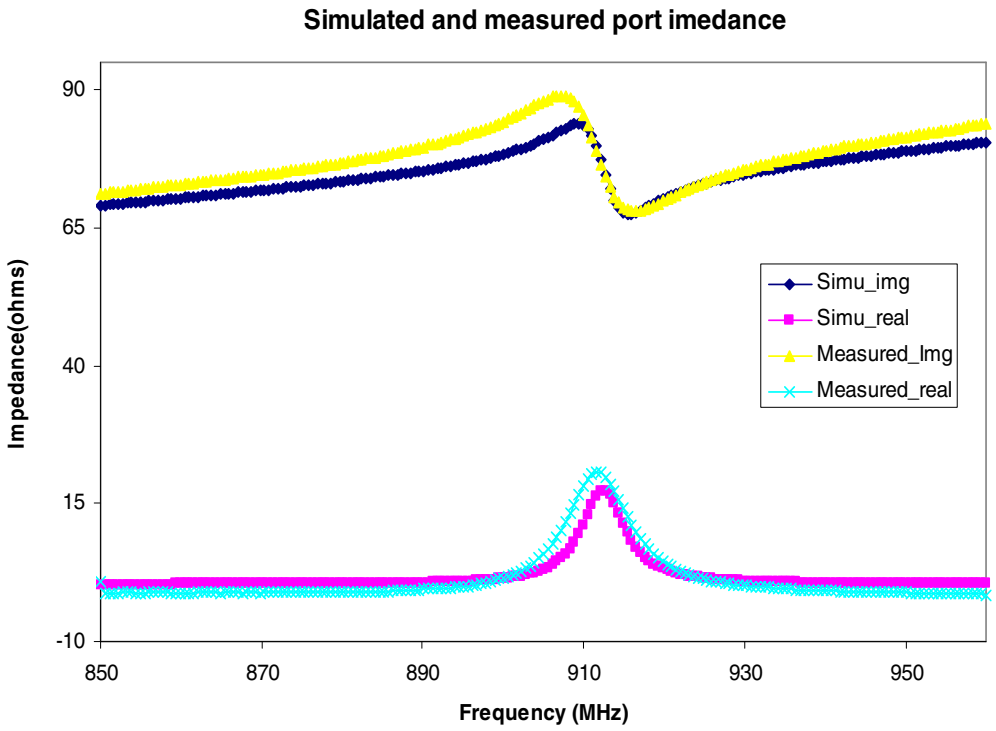


Figure 4.2: Simulated and measured prototype antenna input impedance with single feed excitation.

The above results show that there is good agreement between simulated and measured impedance values. The lower resistance values are nearly equal to zero in simulation, but, measurement shows that they are slightly below zero which in reality is not possible. Since the actual value itself is very small this error is ignored. Since both simulated and measured peaks occur at almost the same frequency and are of equal value it validates our estimates of dielectric constant and loss tangent. The Q-factor of the antenna is as expected. The experimental method used for characterization of substrate materials is therefore accurate.

The gain of the prototype antenna is measured in two different ways. Firstly two prototype antennas are fabricated and tested for input impedance and resonant frequency. Having confirmed that they have similar impedances and resonant frequencies we assume that they will also have similar gains. One antenna treated as the transmitter. It is connected to one of network analyzer ports. The other treated as the receiver is connected to second port of the network analyzer. The ratio of the power transmitted from transmitter antenna to the power received by the receiver antenna is then proportional to the magnitude squared of $S_{21.}$

$$\frac{P_r}{P_t} = \left|S_{21}\right|^2 \tag{4.1}$$

Friis equation can then be re-written as shown.

$$\left|S_{21}\right|^2 = \frac{{G_r}^2 \lambda^2}{(4\pi r)^2} \qquad \Theta\, G_r = G_t \tag{4.2}$$

The antenna gain is then calculated as follows.

$$G_r = \left[\left|S_{21}\right|^2 \frac{(4\pi r)^2}{\lambda^2}\right]^{1/2} \tag{4.3}$$

In an alternate method the prototype is tested in real RFID environment with a programmable RFID reader. The prototype with the RFID IC attached to it is placed in front of the reader antenna at a fixed distance. The reader antenna (transmitter) and the prototype (receiver) have a clear line of sight path. The RFID reader in general is continually hopping i.e., changing frequencies randomly (see Appendix – A for additional information) to different frequencies in the given FCC frequency band. The maximum power for FCC frequency of operation is 36dBm [45]. The reader frequency and its output power can be controlled by setting the appropriate registers in the RFID reader. In testing the prototype tag the RFID reader was programmed to frequency sweep starting from 902.3 MHz to 927.3 MHz in steps of 1 MHz. At each frequency step the output power from the reader is reduced from a maximum allowable of 36 dBm until is reader stops reading the prototype tag. The least reader power at which the tag is read is taken to be the transmit power of the RFID reader that is required to power up the RFID IC.

We assume that the received power from the reader to the tag is the minimum that is required to turn the RFID IC on and is equal to 6.5μm. The RFID transmit antenna is circularly polarized, therefore 3dBi is subtracted from the actual transmit antenna gain to account for the polarization mismatch. Since the RFID IC impedance is matched to the antenna input impedance with less than -10db return loss, we assume that there is no impedance mismatch. Channel conditions are also assumed to be ideal. Using Friis equations we can calculate the receiver antenna gain at each frequency step using the following parameters.

Transmitted power = $P_t$ = minimum reader power required to turn on the RFID IC.

Transmit antenna gain = $G_t$ = 6dBi circular polarization = 3dBi liner polarization.

Received power = $P_r$ = 6.5μW, r = 15 feet.

The antenna gain measured using a network analyzer and the RFID reader are compared against the simulated gain in Figure 4.3. The gain measured using the network analyzer and the RFID reader show the nearly same peak gain as simulated, but the measured bandwidth is significantly larger. The results are summarized in Table 4.1.

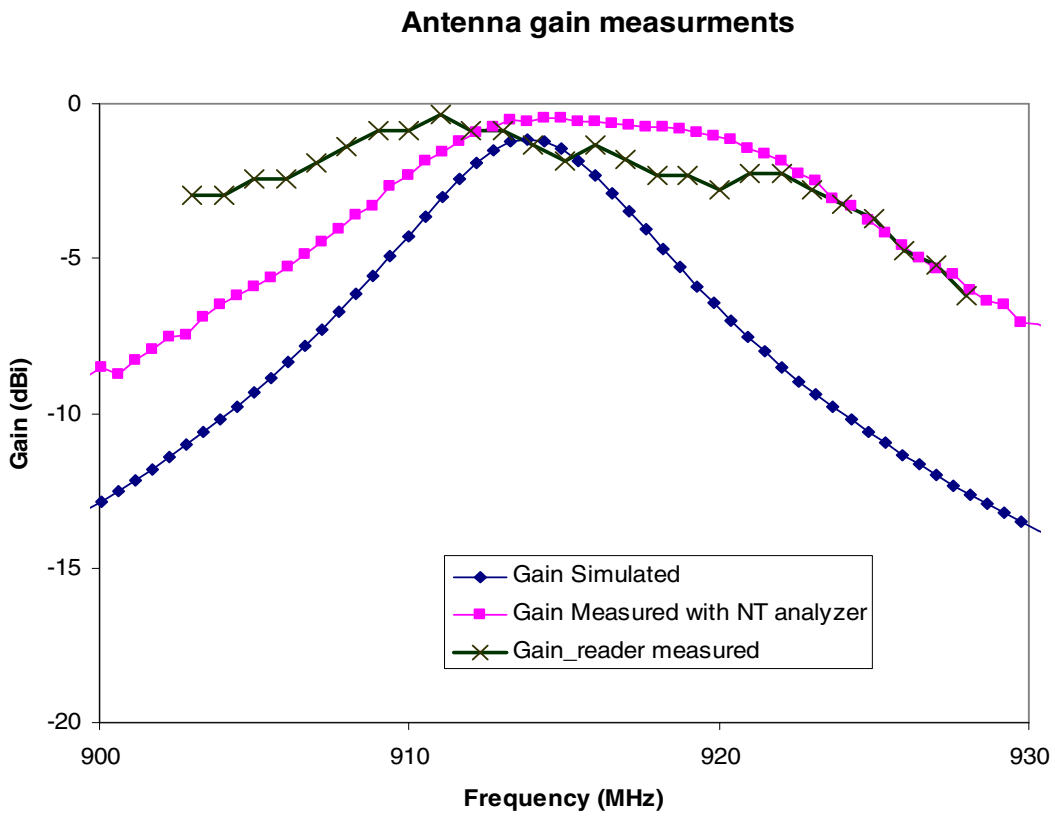


Figure 4.3 Simulated and measured prototype antenna gain characteristics.

| Method | Peak Gain (dBi) | 3dB bandwidth (MHz) |
|---|---|---|
| Simulated | -1.25 | 10.3 |
| Measured with network analyzer | -0.48 | 15.8 |
| Measured with RFID reader | -0.33 | 20.6 |

Table 4.1: Performance characteristics of prototype antenna for different measurement techniques.

While the simulated gain and gain measured with network analyzer differ by 5.5 MHz; the reader measured gain is nearly twice that simulated. The possible reasons for the difference between the simulated and measured values are discussed below.

- The experimental setup to find the dielectric loss tangent of substrate material was inaccurate. If the actual loss tangent is greater than that measured, the Q of the antenna is reduced resulting in greater bandwidth. This may not be true due to fact that the peak gains are still nearly equal. A greater loss tangent must result in reduced peak gain.

- It is quite possible that the antenna has more than one resonance in the desired frequency band due to ground plane resonance i.e., when the ground plane itself acts as a patch and resonates or dielectric resonance i.e., the dielectric cavity between the two conducting planes resonates. This is verified by placing the prototype on a larger sheet of metal and measuring the gain. The results are similar to those obtained previously. This eliminates the possibility of dual resonances.

- Since the RFID IC in strap form is attached to the antenna by conductive epoxy, there is possibility of capacitive coupling between the strap and the antenna. This capacitive bonding between the strap and the antenna could result in increased bandwidth.

- The presence of multipath and ground reflection is ignored in the measurement of prototype antenna gain using both network analyzer and the RFID reader. The measurement was therefore repeated in different physical locations. The results were found to largely coincide with those previously measured. Therefore the effect of channel properties though present, does not account for the increase in the bandwidth of the antenna.

- The reader antenna is assumed to have constant gain over the desired frequency band. A possible variation in the gain with frequency could account for the difference between the gain measured using the network analyzer and the reader antenna. Also any non-linearities in the RFID IC is neglected while measuring with RFID reader.

- Ansoft Designer software tool that is used to simulate these models makes some assumptions in the way it models the antenna design. Anosft Designer assumes an infinite ground plane and substrate over which the patch is created. The Method of Moments (MoM) [46, 47] is used to solve for the electromagnetic (EM) fields of the antenna. This method uses surface waves to model the microstrip patch and polarization currents to model the substrate. The above mentioned assumptions along with the method of computing antenna EM fields could account for deviation of measured gain from simulated gain.

The primary objective of this thesis is to demonstrate that the balanced feed microstrip RFID tag will solve the metal-water problem associated with current passive UHF RFID tags. The prototype is therefore, further tested for performance near metal and water and the results are compared against of some commercially available tags

## 4.2. Comparisons

The prototype tag was compared with other commercial tags in an RFID environment. The prototype and the commercial tags were placed in free space, on metal with cardboard separation, directly on metal, on plastic container with water and the maximum read distance was the metric of interest. We know that when tags are placed on metal radiation resistance increases and on high dielectric they are detuned. The extent of performance degradation is reflected in the reduced read distance.

Several manufacturers have come up with tags that work reasonably well near metal and water, some of these tags were chosen for comparison purposes based on availability at the time of testing.

- Avery metal tag is a dipole design with plexiglass substrate and partial metal ground plane. The tag dimensions are 177 x 25 x 5mm. See Figure 4.4a.
- Symbol RFX3000 is dual dipole design with 5mm foam backing, the overall tag dimensions are 96 x 96 x 5 mm. See Figure 4.4b
- Avery Triflex is also a dual dipole design, with only three poles. One of the poles by symmetry acts as a common base. Tag dimensions are 97 x 107 x 0.07 mm. See Figure 4.4c.

Figure 4.4a Avery metal tag.

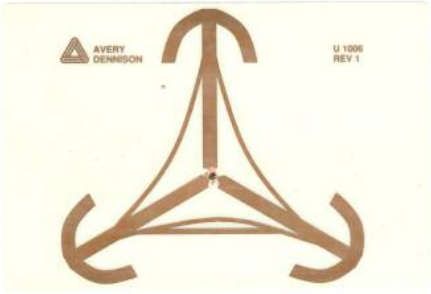


Figure 4.4b: Avery triflex

Figure 4.4c: Symbol RFX3000 with foam backing

The comparison results are summarized in Table 4.2*.

| Tag | Standard | Distance (in ft) | | | |
|---|---|---|---|---|---|
| | | Free space | On metal with 6mm cardboard separation | Directly on metal | Water in plastic container |
| Avery metal tag | EPC 0+ | 12 | 7 | 7 | 5 |
| Avery Triflex | EPC 0+ | 32 | 4 | 0 | 1 |
| Symbol RFX3000 | EPC 0 | 12 | 3 | 2 | 2 |
| Prototype microstrip antenna with balanced | EPC Gen 2 | 32 | 32 | 32 | 32 |

Table 4.2: Performance comparison between prototype and other commercially available tags.

** All tags were tested in the same environment with SAMsys MP9320 v2.8 reader and circularly polarized UHF antenna.*

The above comparisons show that the prototype tag has superior performance in free space as well as near metal and water compared to other tags. The Avery metal tag comes second; this is easily explained by the fact that the Avery metal tag itself is based on microstrip dipole design. It is seen that attaching tags with cardboard separation to metal gives better performance than when attached directly to metal. This is because cardboard has dielectric constant equal to nearly that of free space and placing the tag with cardboard separation gives reduced radiation resistance than compared to tag directly on metal, resulting in better impedance match and therefore better read distance. Unlike other tags the prototype does not lose any performance in the presence of metal or water.

*5.*

# Chapter 5

# Future work

The balanced feed matching network microstrip antenna is a potential solution to the metal-water problem of RFID. The results from chapter 4 however show that the single patch single shorting stub design is limited in its performance by narrow gain bandwidth. The constraint to keep the microstrip RFID tag low profile and cost effective, eliminates the possibility of making use of traditional broadband techniques such as proximity coupling, thick substrates, and, stacked patches. The scope of future work lies in exploring planar mechanisms that would allow us to increase the gain bandwidth and reduce the form factor. One of the possible techniques is to use multiple, narrow rectangular patches of different lengths to create multiple resonances at the desired frequencies. This however necessitates the increase in the form factor due to the presence of two patches and consequently two matching networks.

In this chapter we investigate some of novel feed mechanisms and coupling techniques that will allow us to use a 2 element planar microstrip antenna array that extends the bandwidth of the antenna without necessitating any increase in substrate thickness or the form factor of the antenna. Simulation results are also presented. While the 2 element array resolves the bandwidth issue to an extent, the large form factor issue remains. Towards the end of this chapter design techniques using meandered patch geometries, capable of multiple modes [32] for multi-resonance are suggested to reduce the form factor while simultaneously

increasing the bandwidth. There is also a need to study the effects of balanced feed mechanism on a microstrip patch and create mathematical models that could describe the relation between antenna performance and feed parameters, and allow optimization based on derived theoretical limits.

## 5.1. Broadband designs

### 5.1.1. Dual patch broadband antenna design

The simplest way to create a broadband antenna is to make an array of elements [34] that will couple and resonate at different intervals in the desired frequency band, providing an overall 3dB bandwidth that is greater when compared to that of a single resonating element. The antenna array construction is very similar to that of a single element patch expect for the feed mechanism. The feed structure is now constructed such that it couples to both elements and provides an impedance bandwidth that is greater than or equal to the gain bandwidth of the array. The antenna is excited either by means of dual transmission lines that form a balanced feed structure or by means of inductive couple feed. The feed mechanisms can be classified into three categories as follows.

- Direct balanced feed
- Inductively coupled feed
- Combined inductive and direct feed

The dual patch microstrip antenna design is often capable of dual resonance and in some cases can give rise to multiple (tri or quadruple) resonances. Some of the design instantiations based on the above feed methods with EPC Class 1 Gen 2 RFID IC with 62

mil polypropylene (PP) substrate, $\varepsilon_r = 2.265$, $\tan \delta = 0.0035$ are discussed below. We choose polypropylene for these designs as we know that it has very low loss tangent and therefore is a high Q- factor device. The idea is to see by what amount, the 3dB bandwidth of a high-Q antenna can be increased using the above mentioned techniques.

*Dual patch direct balanced feed:* The fundamental concept of a balanced microstrip feed to a rectangular patch is extended to two rectangular patches in this example. The design consists of two patches, coupling between which plays an important role in determining the resonant frequencies and the overall bandwidth of the array. Spacing the array elements too far results in under coupling, narrow gaps could result in over coupling and the antenna efficiency is reduced in both cases.

While critical coupling between array elements is important, the design of the matching network also affects the resonant frequency (Refer section 3.3.2). We therefore create two matching networks allowing greater degree of freedom in design. The design uses two patches with dissimilar dimensions; each having a pair of differential feed transmission lines connecting it to the RFID IC through a single shorting stub matching network. Figure 5.1 shows the simulation model of the dual patch direct feed design. The overall dimensions of the antenna are 112mm x 49mm and it is implemented on PP substrate. The antenna array has two operating frequencies corresponding to 914 MHz and 926 MHz. The antenna has a 3dB BW of 4.2 MHz from 911.7 to 915.9MHz and 4 MHz from 924.5 to 928.5 MHz. The overall BW is hence equal to 8.2 MHz i.e. twice the bandwidth of a single resonant patch with same substrate.

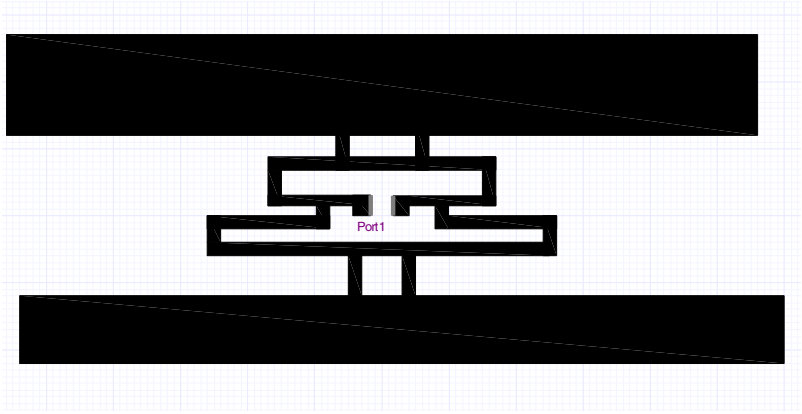


Figure 5.1: Simulation model for dual patch direct feed broadband design.

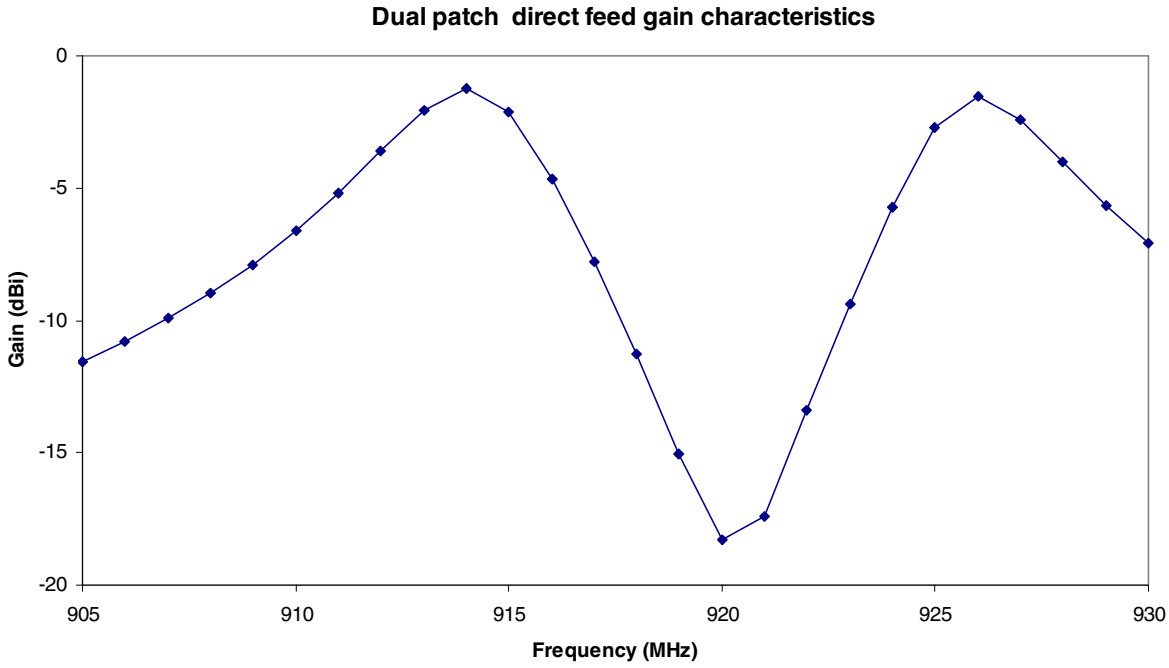


Figure 5.2: Simulated gain vs frequency – Direct feed.

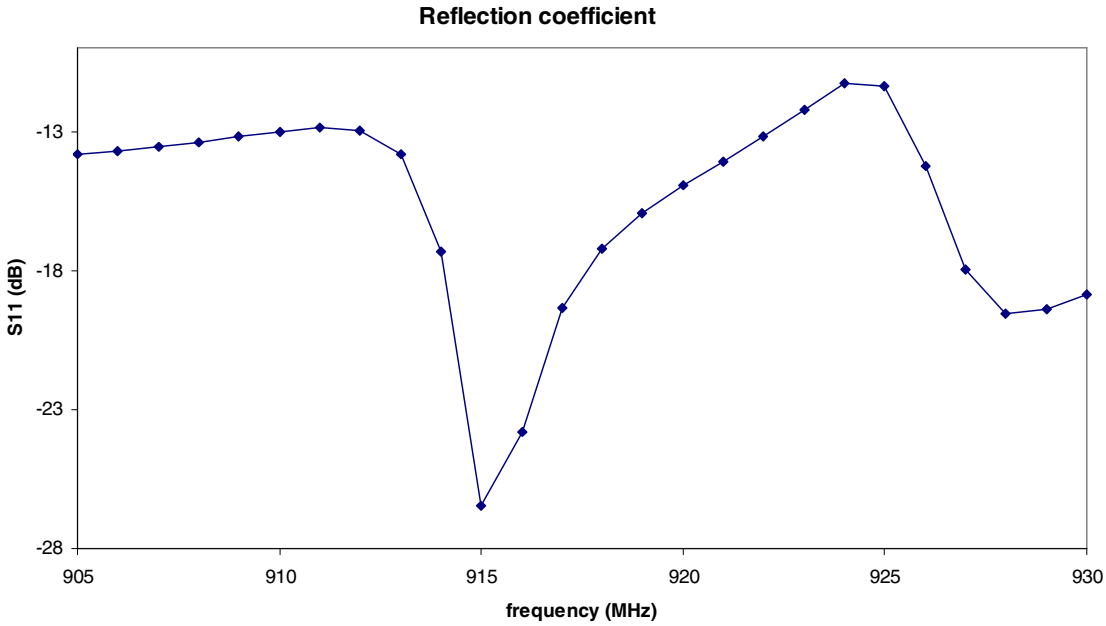


Figure 5.3: Simulated reflection coefficient vs frequency – Direct feed.

The dual patch dual direct feed design, as this is called, was primarily intended to create two narrow gain peaks, we however observed that the matching network can be elongated to create a loop that could add a third resonance. Here the shorting stub matching network along with the balanced feed transmission line acts as a loop antenna, with effective electrical length of $0.49\lambda_{eff}$ at 915 MHz. The overall antenna physical dimension is 110mm x 58mm. The antenna design and its performance characteristics are shown in Figures 5.4 to 5.6.

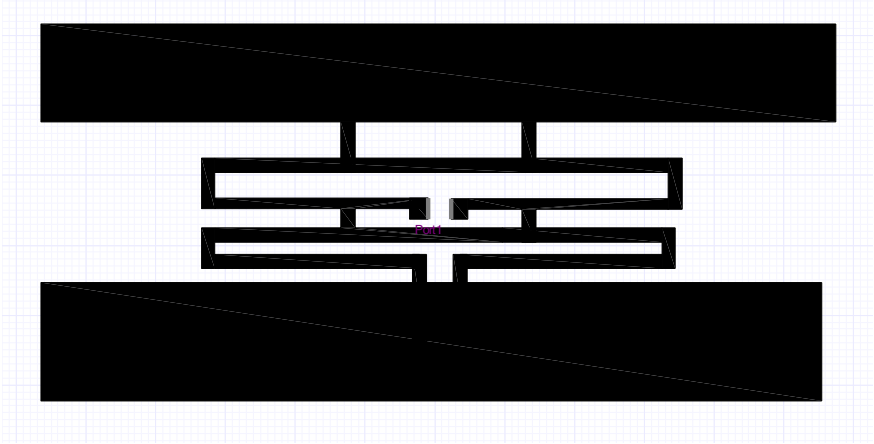


Figure 5.4 : Simulation model for dual patch direct feed tri- resonant broadband design

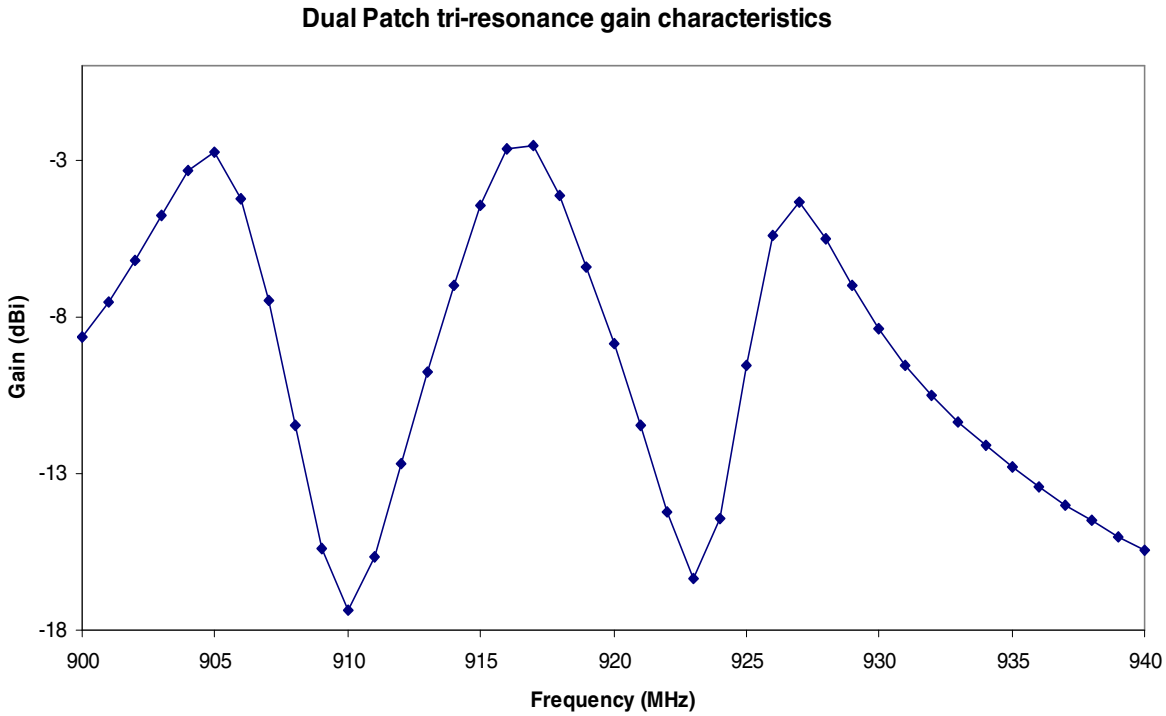


Figure 5.5: Simulated gain vs frequency – Tri – resonance.

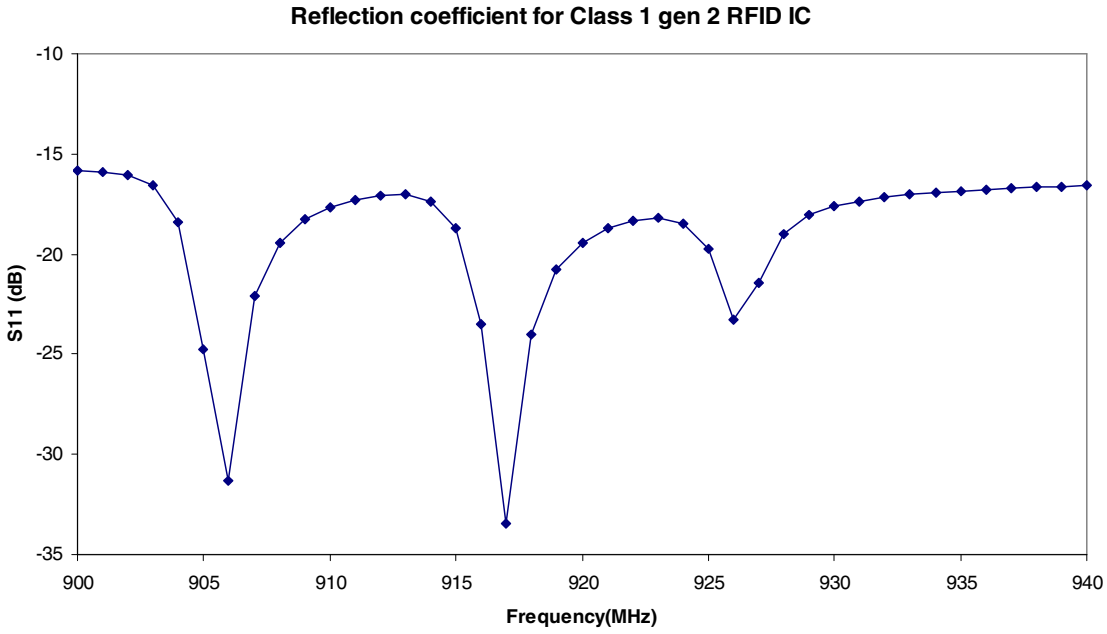


Figure 5.6: Simulated reflection coefficient vs frequency – Tri – resonance.

The dual patch tri-resonant antenna has three gains peaks with frequencies corresponding to 905, 915 and 925 MHz respectively. The 3dB BW corresponding to the peaks are 4.5 MHz from 902 to 906.5 MHz 8.6 MHz from 914 to 918.6 MHz and 3.5 MHz from 925.5 to 929 MHz. The overall 3dB BW is the sum of the individual bandwidths and is equal to 12.6 MHz. Multiple peaks allow us to operate in different narrow ISM bands.

*Dual patch inductive feed:* While the dual patch direct feed design allows us to double or triple the bandwidth as the case might be, still requires the construction of two matching networks that occupies considerable area. The form factor therefore remains large. Replacing the direct balanced feed transmission lines with an inductively coupled feed reduces the matching network complexity considerably.

Inductive feed mechanism to two rectangular patches uses a folded transmission line length to create the impedance match, while coupling to patches. Since the feed line itself is purely inductive, matching to large reactive impedance is easier than compared to a direct feed. The inductive feed transmission line eliminates the need for a shorting stub. The design uses two rectangular patches, the overall dimensions of the antenna being 110mm x 40mm. Two narrow transmission lines connect to each patch enable the feed to inductively couple to the patch with increased coupling efficiency. The peak gain occurs at 915 MHz and 950 MHz. The 3 dB bandwidth is 10.5 MHz.

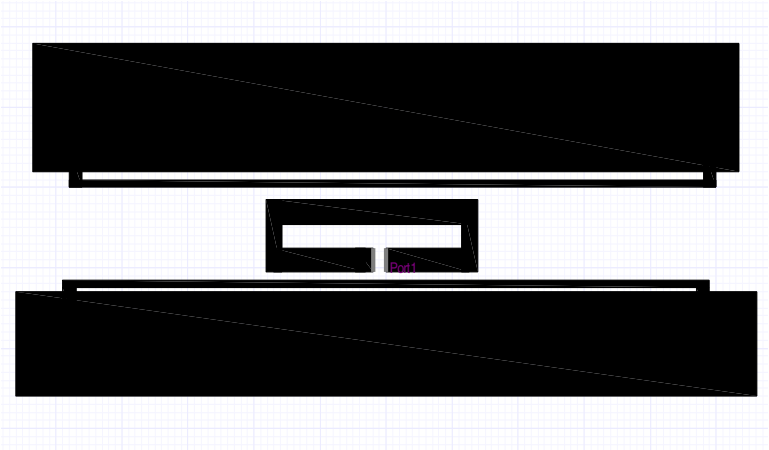


Figure 5.7: Simulation model for dual patch inductive feed broadband design.

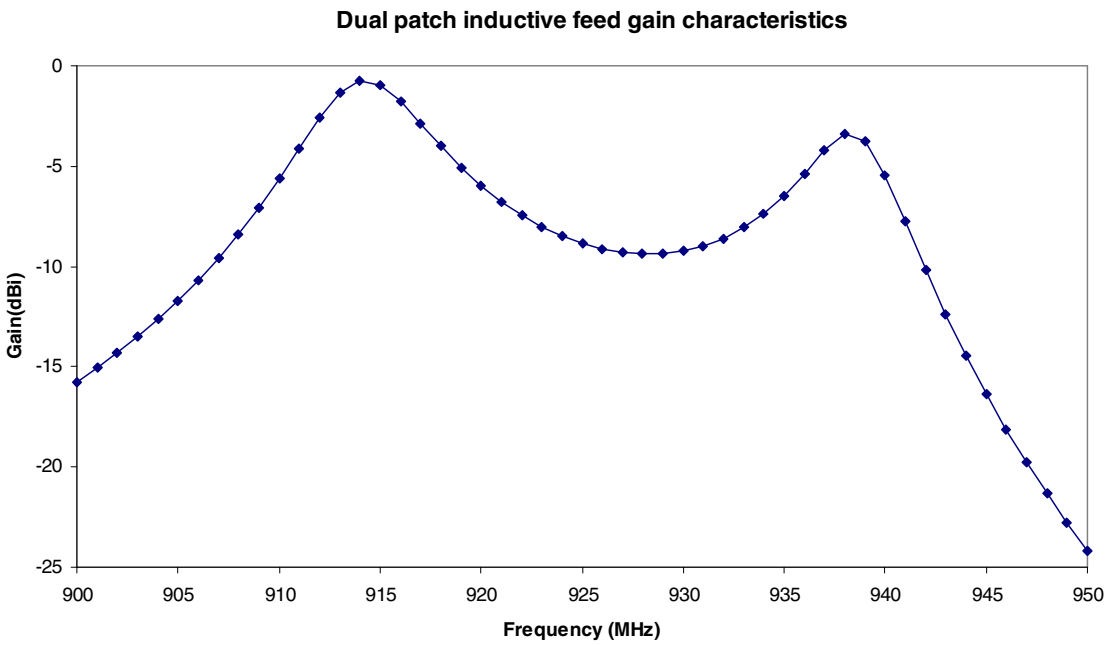


Figure 5.8: Simulated gain vs frequency – Inductive feed.

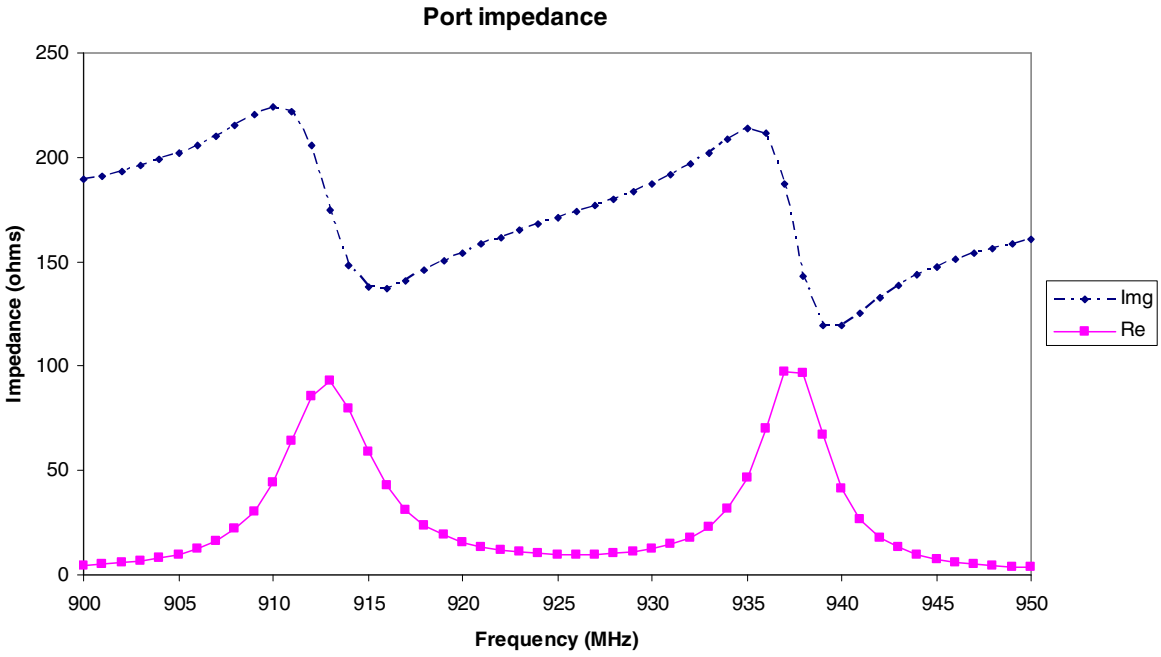


Figure 5.9: Simulated impedance vs frequency – Inductive feed.

While dual patch inductive feed is an improvement over the single patch and the dual patch direct feed designs, it suffers from a very low gain between the resonant peaks. This is due

the induced currents in the coupled patches flowing in opposite directions resulting in loss of radiated power.

The above implementations are useful in operating over multiple narrow ISM frequencies, like ETSI (865-868 MHz), Japan (953-956) etc. In operating over FCC, which has a bandwidth of 28 MHz, from 902 to 930 MHz, these designs cover only one third of the available bandwidth. With RFID readers frequency hoping over the entire bandwidth, tags that have selective response regions (i.e. narrow peak gain followed by low gain regions) such as the above could result in reduced number of reads at a fixed distance. Maintaining an acceptable minimum gain over the entire bandwidth is necessary to overcome this problem. The dual patch combined inductive and direct feed achieves this performance.

*Dual patch combined feed:* Combining the techniques of direct and inductive feed enables us to critically couple to both the elements of the array without canceling the currents severely. In this design one patch is connected to a pair of transmission lines that act as a balanced feed. A short circuit stub is connected across the feed lines. The section of balanced feed line below the shorting stub and the shorting stub itself form an inductive loop that couples with the second patch. The effects of coupling and transmission line length on resonant frequency are not well understood, the design therefore is manually tuned based on simulations to achieve the right frequencies of resonance and impedance match. Figure 5.10 shows the simulation model and Figures 5.11 and 5.12 show the performance characteristics.

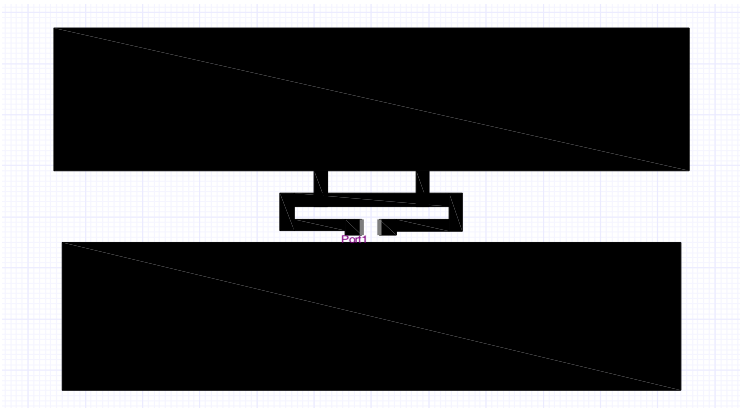

Figure 5.10: Simulation model for dual patch combined feed broadband design.

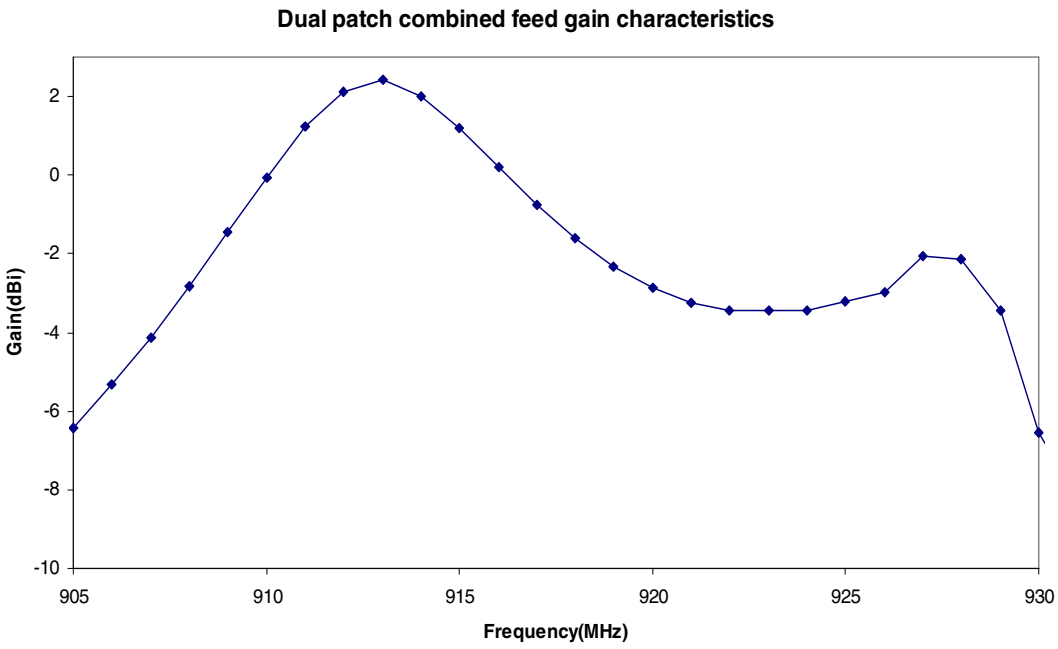


Figure 5.11: Simulated gain vs frequency – Combined feed.

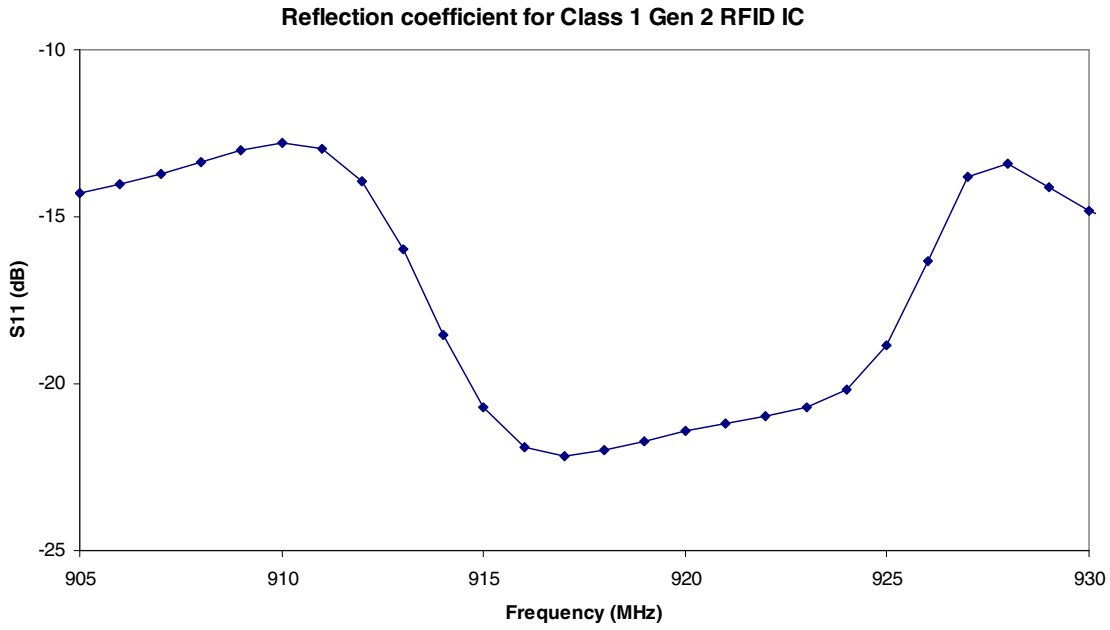


Figure 5.12: Simulated reflection coefficient vs frequency – Combined feed.

The antenna is designed to have a primary peak at 913.5MHz and a secondary peak at 927.5 MHz. The gain between 906 to 929 MHz is maintained within -6.5 dBi of peak gain (i.e. above the minimum acceptable gain of -5 dBi). The 3dB BW of this antenna for the primary peak alone is found to be 7MHz from 910 to 917MHz. For 23 MHz the gain remains above the minimum acceptable level covering 82% of the FCC bandwidth. The antenna dimensions however, are larger than any of the previous implementations at 111mm x 70 mm.

### 5.1.2. Multi-mode multi-resonant design

The dual patch broadband design enables us to overcome the narrow bandwidth problem without significant increase in the form factor. It does not however provide a solution to

creating small metal mountable broadband RFID tags. Using meandered transmission lines can effectively reduce the physical dimension of the antenna, the gain bandwidth of the antenna will however be severely reduced as aperture is reduced. It is necessary at this point to recall that we can extend the principle of balanced feed mechanism to all symmetric microstrip patch geometries discussed in Section 2.4.1.

Microstrip patches geometries such as a square, circle, ring that have bilateral symmetry are capable of multiple modes of operation as they can have more than one pair of radiating edges depending on the electrical length and the current flow direction. Using these geometries with slots to reduce the physical size, while generating multiple modes could effectively combat both the bandwidth and the form factor problem associated with planar microstrip RFID tags.

There is immense scope in exploring new designs that will use coupled feed mechanisms with meandered patch geometries to further reduce matching network size and complexity. There is a need to also thoroughly investigate the effects of planar balanced feed mechanism on the microstrip patch, which will enable us to analytically determine the critical parameters such as the feed line characteristics and matching network design to achieve optimum performance under the constraints of low profile substrate, small form factor and cost effective implementation. More rigorous test procedures need to be developed to test and analyze the performance characteristics of these designs.

# Chapter 6

# Conclusions

The research motivation for this thesis was to show that a microstrip antenna can be designed with dual feed transmission lines resulting in a balanced feed. The microstrip antenna thus designed is completely planar in nature and does not have any cross-layered structures. The theory for the design of a balanced feed microstrip antenna stems from the traditional odd mode symmetry of the design analysis that allows us to simplify the balanced feed design to the well understood, single microstripline feed. Odd mode analysis alone is therefore sufficient to describe the working of the microstrip antenna with balanced feed mechanism.

The primary application for this type of microstrip antenna is in the field of RFID implementation where a cost effective solution to identify and track metal and high dielectric materials was necessary. The planar microstrip antenna with balanced feed eliminates the need for any cross–layered structures such as vias or shorting walls in the construction of a microstrip RFID tag and thus reduces the manufacturing complexity and therefore the cost associated with existing microstrip RFID solutions.

The balanced feed microstrip antenna was implemented using readily available materials that were characterized in the lab by experimental methods. The design consisted of a an antenna with shorting stub matching circuit to for impedance matching to the RFID IC on high density polyethylene substrate and a ground plane. The effects of various design parameters

were first analyzed by extensive simulations, an initial set of values were selected based on these studies as the starting point for the microstrip antenna design.

Initial design was single microstrip patch antenna with dual shorting stub matching network, further experimentation showed that the similar results could be achieved with a single shorting stub matching network, thus reducing form-factor and design complexity. Optimization of the design is seen to involve numerous tradeoffs due to fact that the effects design parameters are inter related and there is no specific optimization rule. The constraints of low profile and small form-factor under which the antenna was designed limited the extent to which antenna efficiency and bandwidth could be increased. The final design of the microstrip antenna with balanced feed was made to operate in FCC RFID frequencies with peak performance of -1.25dBi at 915 MHz. In order to validate the simulation results a prototype was fabricated and its characteristics were experimentally measured using standard lab equipment as well as with the application oriented RFID setup. Our measurements while validating the simulation results to a larger extent showed better gain characteristics than expected. We realize that there are certain inaccuracies and assumptions on which the simulated and measure results are based that could result in this difference between simulation and measurement.

A comparison with some of the existing UHF RFID tags has proved that our design is capable of achieving consistent performance when attached to any material. Our prototype tag had greater free space performance than any other tag, and maintained the performance even when placed on metal sheets or containers with high dielectric substances like water.

The optimized microstrip antenna with balanced feed mechanism of UHF RFID proposed in this thesis provides an attractive solution to the metal-water problem associated with passive UHF RFID tags. The over all performance of the prototype was satisfactory and the design goals were achieved, the concept of microstrip patch antenna with balanced feed mechanism is therefore considered to be successfully implemented and tested. It however is not the complete solution in itself as it suffers from narrow bandwidth, cannot be operated in ISM bands worldwide, and, is not nearly as small in size as desired for certain applications.

We explored some broadband techniques that could be used to overcome the problems associated with the current design. Dual patch with direct and coupled fed techniques were designed and found to have more than twice the bandwidth that could be achieved with a single patch design. It was also noted that development of mathematical models to predict the effects of various parameter values on the antenna performance is necessary along with a thorough procedures to test and validate the designs. The fact that industry needs are yet to be fully addressed shows that further research initiatives are need in this direction.

# References


[1] Kwon, H. and Lee B.: 'Compact slotted planar inverted-F RFID tag mountable on metallic objects.' IEEE Electronics Letters, November 2005, Vol. 41, pp1308-1310.

[2] Ukkonen, L., Engels, D., Sydanheimo, L., and Kivikoski, M.: 'Planar wire-type inverted-F RFID tag antenna mountable on metallic objects.' IEEE Int. Symp. on AP-S, June 2004, Vol. 1, pp. 101–104.

[3] Choi, W., Son, H. W., Ji-Hoon Bae, Choi, Y. G., Cheol Sig Pyo and Jong Suk Chae: 'An RFID tag using a planar Inverted F antenna capable of being stuck to metallic objects.' ETRI Journal, April 2006, Vol. 28, No. 2, pp 216-218.

[4] Carl Mueller, Introduction to RFID, March 2004, http://www.corefunction.com/resources/wp/introduction_rfid.pdf

[5] FKI logistics, RFID for the Real World, 2005,

[6] Laran RFID, Basic introduction to RFID technology and its use in supply chains, White paper , April 2004.

[7] Jim Eagleson, RFID: The Early Years, 1980 – 1990, http://members.surfbest.net/eaglesnest/rfidhist.htm

[8] Symbol Technology, Understanding the Key Issues in Radio Frequency Identification (RFID), White paper, 2004.

[9] Logistics and material readiness, home page: http://www.acq.osd.mil/log/rfid/index.htm, 2005.

[10] Wynne, M. W., Radio frequency identification (RFID) policy. Policy statement, The Under Secretary of Defense, July 30 2004.

[11] Ann Marie Phaneuf, Meeting The EPC RFID Mandates: Where To Begin, Weber Marketing Systems Inc., White paper

[12] Ahmed ElAmin, RFID advances help food traceability, http://www.foodnavigator-usa.com/news/ng.asp?id=65062-idtechex-rfid-traceability, 2006

[13] RFSAW, The Global SAW Tag – A New Technical Approach to RFID, White paper, 2004

[14] Ramakrishnan K. N. M.: 'Performance Benchmarks for Passive UHF RFID Tags.' Masters Thesis report, 2005

[15] Finkenzeller K., RFID Handbook, Wiley & Sons, 2 edition, 2003.

[16] Definition of Inductive coupling, http://en.wikipedia.org/wiki/Inductive_coupling , 2006.

[17] Sarma, S. and Engels, D. W., On the future of RFID tags and protocols, White paper, Auto-ID Center, Massachusetts Institute of Technology, 2003.

[18] Powell K., Passive Radio Frequency Identification – A Primer for New RF Regulations, Matrics, 2003.

[19] Balanis, C.A., Antenna Theory: Analysis and Design, John Wiley & Sons, Inc, 1997.

[20] Stutzman, W.L., and Thiele, G.A., Antenna Theory and Design, John Wiley & Sons, Inc, 1998.

[21] Lo, Y. T., and Lee S. W., Antenna handbook: Antenna theory, Vol.2, International Thompson Publishing, Inc, 1993.

[22] Glover, B., and Bhatt, H., RFID Essentials, O'Reilly Media, Inc, 2006

[23] Catherine, M.: 'Symbol Announces Gen 2 Tags, Converter Program.' RFID Journal, News article, May 2006.

[24] Alien Technology – RFID tags, http://www.alientechnology.com/products/rfid_tags.php

[25] Avery Dennison RFID: Products: Portfolio, http://www.rfid.averydennison.com/us/products_portfolio.php

[26] Deschamps, G. A.: 'Microstrip Microwave Antennas.' The 3rd Symp. on The USFA Antenna Research and Development Program, University of Illinois Monticello, Illinois, October 1953.

[27] Hirvonen, M., Pursula, P., Jaakkola, K., and Laukkanen, K.: 'Planar inverted-F antenna for radio frequency identification.' IEEE Electronic letters. 2004, Vol. 40, pp. 848–850.

[28] Bhattacharyya, A. K., and Garg, R.: 'Generalised transmission line model for microstrip patches.' IEE Proceedings, 1985, Vol. 132, pp. 93–98.

[29] Derneryd A.G.: 'Linearly Polarized Microstrip Antennas.' IEEE Trans. on AP, November 1976, Vol. AP-24, pp. 846 – 851.

[30] Lo, Y. T., Solomon, D., and Richards W.F.: 'Theory and Experiment on Microstrip antennas.' IEEE Trans. on AP, 1979, Vol. AP-27, pp. 137 – 149.

[31] Richards W.F., Lo, Y. T., and Harrison D. D.: 'An Improved theory for Microstrip antennas and Application.' IEEE Trans. on AP, 1981, Vol. AP-29, pp. 38 – 46.

[32] Garg, R., Bhartia, P., Bahl, I., and Ittipiboon, A., Microstrip Antenna Design Handbook, Artech House, Inc, 2001.

[33] Nakar, P. S.: 'Design of a compact Microstrip Patch Antenna for use in Wireless/Cellular Devices.' Masters Thesis report, 2004.

[34] Kumar, G., and Ray, K.P., Broadband Microstrip Antennas, Artech House, Inc, 2003.

[35] Waterhouse, B. R., Microstrip Patch Antennas: A Designer's Guide, Kluwer Academic Publishers, 2003.

[36] Bancroft, R., Microstrip and Printed Antenna Design, Noble Publishing Corporation, 2004.

[37] Definition of Inverted-F antenna, www.qsl.net/kb7qhc/**antenna**/Inverted%20F/index.htm , 2006.

[38] Pozar, D. M., Microwave Engineering, Second Edition, John Wiley & Sons, Inc, 1988.

[39] ST Micro, XRA00 UHF EPCglobal Class 1b Contactless Memory Chip 96 bit ePC with Inventory and Kill Function, Technical report, 2005.

[40] Imping RFID Technology Series, The RFID Antenna: Maximum Power Transfer, Technical report, 2005.

[41] Definition of dielectric constant, http://www.answers.com/topic/dielectric-constant , 2006

[42] Integrated publishing, Electrical Engineering Training series, Dielectric losses, http://www.tpub.com/content/neets/14182/css/14182_116.htm , 2006

[43] Definition of Loss tangent, http://www.rfcafe.com/references/electrical/dielectric_constants_strengths.htm , 2006

[44] Gonzalo, R., P. de Maagt, and Sorolla, M.: 'Enhanced Patch-Antenna Performance by Suppressing Surface waves Using Photonic-Bandgap Substrates.' IEEE Trans. Microwave theory and techniques, 1999, Vol. MTT- 47, pp. 2131 – 2138.

[45] SAMSys Technologies, Inc, SAMSys MP9320 UHF Reader - Field Installation and Calibration Guide, 2005.

[46] Newman, E.H. and Tylyathan, P., "Analysis of Microstrip Antennas Using Moment Methods." IEEE Trans. on AP., January 1981, Vol. AP-29, No. 1, pp. 47-53.

[47] Harrington. R.F., Field Computation by Moment Methods, Macmillan, New York, 1968.

# Appendix - A

The frequency bands used in different countries for passive UHF RFID are as detailed in Table A1.

Table A1: Frequency band of RFID operation in different countries

| Country | Frequency of operation |
|---|---|
| Federal Communications commission (FCC) - USA and Canada | 902-928MHz |
| Korean frequency | 910-914 MHz |
| Korean and Singapore frequency | 923-925 MHz |
| Hong Kong frequency | 920-925 MHz |
| European Telecommunications Standards Institute (ETSI ) - Europe | 865-868MHz |

Table A1: Frequency band of RFID operation in different countries

The SAMsys MP9320 v2.8 reader and circularly polarized UHF antenna was used in this thesis for all tag – reader measurements. The reader uses a combination of TPC register and the VFx registers [45] for frequency hopping in a particular frequency band. The FCC and ETSI frequency hopping tables are given in Table A2 and Table A3 respectively

Table A2: FCC frequency hopping table

| Index | Frequency in (MHz) | | | | | | |
|---|---|---|---|---|---|---|---|
| 1 | 902.100 | 34 | 908.700 | 67 | 915.300 | 100 | 921.900 |
| 2 | 902.300 | 35 | 908.900 | 68 | 915.500 | 101 | 922.100 |
| 3 | 902.500 | 36 | 909.100 | 69 | 915.700 | 102 | 922.300 |
| 4 | 902.700 | 37 | 909.300 | 70 | 915.900 | 103 | 922.500 |
| 5 | 902.900 | 38 | 909.500 | 71 | 916.100 | 104 | 922.700 |
| 6 | 903.100 | 39 | 909.700 | 72 | 916.300 | 105 | 922.900 |
| 7 | 903.300 | 40 | 909.900 | 73 | 916.500 | 106 | 923.100 |
| 8 | 903.500 | 41 | 910.100 | 74 | 916.700 | 107 | 923.300 |
| 9 | 903.700 | 42 | 910.300 | 75 | 916.900 | 108 | 923.500 |
| 10 | 903.900 | 43 | 910.500 | 76 | 917.100 | 109 | 923.700 |
| 11 | 904.100 | 44 | 910.700 | 77 | 917.300 | 110 | 923.900 |
| 12 | 904.300 | 45 | 910.900 | 78 | 917.500 | 111 | 924.100 |
| 13 | 904.500 | 46 | 911.100 | 79 | 917.700 | 112 | 924.300 |
| 14 | 904.700 | 47 | 911.300 | 80 | 917.900 | 113 | 924.500 |
| 15 | 904.900 | 48 | 911.500 | 81 | 918.100 | 114 | 924.700 |
| 16 | 905.100 | 49 | 911.700 | 82 | 918.300 | 115 | 924.900 |
| 17 | 905.300 | 50 | 911.900 | 83 | 918.500 | 116 | 925.100 |
| 18 | 905.500 | 51 | 912.100 | 84 | 918.700 | 117 | 925.300 |
| 19 | 905.700 | 52 | 912.300 | 85 | 918.900 | 118 | 925.500 |
| 20 | 905.900 | 53 | 912.500 | 86 | 919.100 | 119 | 925.700 |
| 21 | 906.100 | 54 | 912.700 | 87 | 919.300 | 120 | 925.900 |
| 22 | 906.300 | 55 | 912.900 | 88 | 919.500 | 121 | 926.100 |
| 23 | 906.500 | 56 | 913.100 | 89 | 919.700 | 122 | 926.300 |
| 24 | 906.700 | 57 | 913.300 | 90 | 919.900 | 123 | 926.500 |
| 25 | 906.900 | 58 | 913.500 | 91 | 920.100 | 124 | 926.700 |
| 26 | 907.100 | 59 | 913.700 | 92 | 920.300 | 125 | 926.900 |
| 27 | 907.300 | 60 | 913.900 | 93 | 920.500 | 126 | 927.100 |
| 28 | 907.500 | 61 | 914.100 | 94 | 920.700 | 127 | 927.300 |
| 29 | 907.700 | 62 | 914.300 | 95 | 920.900 | 128 | 927.500 |
| 30 | 907.900 | 63 | 914.500 | 96 | 921.100 | 129 | 927.700 |
| 31 | 908.100 | 64 | 914.700 | 97 | 921.300 | 130 | 927.900 |
| 32 | 908.300 | 65 | 914.900 | 98 | 921.500 | | |
| 33 | 908.500 | 66 | 915.100 | 99 | 921.700 | | |

Table A3: ETSI Frequency hopping table

| **Index** | **Frequency (MHz)** |
|---|---|
| 1 | 865.100 |
| 2 | 865.300 |
| 3 | 865.500 |
| 4 | 865.700 |
| 5 | 865.900 |
| 6 | 866.100 |
| 7 | 866.300 |
| 8 | 866.500 |
| 9 | 866.700 |
| 10 | 866.900 |
| 11 | 867.100 |
| 12 | 867.300 |
| 13 | 867.500 |
| 14 | 867.700 |
| 15 | 867.900 |